

Response to Reviewers Document for “Long-Term Global Ground Heat Flux and Continental Heat Storage from Geothermal Data” by Francisco José Cuesta-Valero, Almudena García-García, Hugo Beltrami, Fidel González-Rouco and Elena García-Bustamante.

We thank the Reviewers for their thoughtful and constructive feedback.

This Response to Reviewers file provides a complete documentation of the changes made in response to each individual Reviewer’s comment. Reviewers’ comments are shown in plain text. Author responses are shown in bold blue text. Corrections within the revised manuscript are shown in blue text. All line numbers in this file refer to locations in the revised manuscript with changes marked unless indicated otherwise.

#####

Reviewer #1

Summary:

The manuscript presents an estimation of past ground heat flux and past surface temperatures over the last few centuries based on measured borehole temperature profiles. The main objective of the analysis is to estimate the history of vertical heat flux into the ground, in the more general framework of the global energy fluxes perturbed by anthropogenic climate change. The methodology of deriving past surface temperatures from borehole temperature profiles is well established. The novelty in this study is threefold: the shifted focus towards the surface heat fluxes, the estimation of uncertainties, and the expansion of the available data base. The main conclusion is that the ground heat flux estimate from borehole profiles has larger than had previously estimated. The authors claim that this component of the energy fluxes is important within the climate system.

Recommendation:

Some revisions necessary, but I think this is a valuable contribution to Climate of the Past. The manuscript is generally well written - although some sections would benefit from a revision.

General comments:

1) I found Section 2 too detailed. It will certainly help readers with a more superficial background on borehole climatology, but I think that this section can be compressed, displaying the main ideas and the important technical details that are used later on in the manuscript. For instance, I do not think it is necessary to display equation 11 in such level of detail. A matrix equation should suffice.

Indeed, Section 2 consists of a detailed description of borehole methodology. We have reduced the level of detail in Section 2.3 as suggested by the reviewer, although the rest

of Section 2 only contains minor adjustments, since we described the most important concepts of borehole climatology to improve the overall clarity and reproducibility of the work described in the article.

2) In contrast, section 3 should include the new methodological aspects of the direct heat flux inversion. Here, either I missed something or something is indeed missing. On the one hand, the manuscript alludes to a direct inversion of the flux profiles (equation 18) to heat flux histories, using also the Perturbed Parameter approach (line 266) But the methodology for the direct inversion of heat flux histories is not explained, at least I could not find it in the manuscript. The PPI approach has been explained for the temperature inversions, not the heat flux inversions. Perhaps, it is so obvious that it does not need an explanation, but to me it is not that clear. In case I misunderstood something here, it is likely than an average reader will also get confused. There is an imbalance between the level of detail presented for the temperature history inversions and for the heat flux inversions.

The inversion method used to retrieve ground heat flux histories from heat flux profiles is the same as the one for estimating ground surface temperature histories from temperature profiles. Hence, we described both inversion procedures in the same section (Section 3.3.2). Nevertheless, we agree with the reviewer about the confusion that this may cause on the reader. Thus, we have rearranged the text into two specific sections on the new version of the manuscript, one for describing the inversion of temperature profiles, and another one for describing the inversion of heat flux profiles (Sections 3.3.2 and 3.3.3, respectively).

On the other hand, the manuscript also used ground heat flux histories derived from the inversion of ground temperature histories, equation (19). There are then apparently two reconstructions of the ground heat flux histories, one by a 'direct inversion method' and one based on the reconstructed surface temperatures. And yet a third estimation for the recent period using the CRU temperatures. If this is true, it should be clearly indicated. Please consider labeling these three products to guide the reader.

We have changed the confusing terms on the text, figures and tables, incorporating the variable and the method used to obtain the variable in the name of each estimate. Thus, the temperature and flux data from the CRU product are now named SAT_CRU and GHF_CRU, respectively; the temperature, flux and heat estimates from borehole temperature profiles using the Standard method are named GST_Standard, GHF_Standard and GHC_Standard, respectively; the temperature, flux and heat estimates from borehole temperature profiles using the PPI method are named GST_PPIT, GHF_PPIT and GHC_PPIT, respectively; and the flux and heat estimates from borehole flux profiles using the PPI method are named GHF_PPIF and GHC_PPIF, respectively. We have also included a new appendix including the definition of all these acronyms (Appendix A, page 17).

3) The approach leading to the weighting scheme in equation 17 can be problematic. I am not saying it is wrong, but a more versed statistician than me may complain. In essence, what the authors are doing is applying Bayesian scheme to estimate the inversion uncertainties. They assume a prior distribution of some model parameters, which are then passed through the model to produce temperature profiles, and these synthetic profiles are weighted by the likelihood (17). The problem is that there are hidden assumptions in this approach that are not explicitly stated. Are the initial model parameters a priori equally probable? Without that assumption it is not possible to attach posterior probabilities to the synthetic profiles and to the model parameters. A more sophisticated, fully Bayesian approach could include a Monte Carlo Markov chain sampling of those posterior probabilities and of the temperature histories, in which their values are varied in a more systematic scheme. In any case, the hidden assumptions that authors are making about the relative probabilities of the assumed model parameters need to explicitly stated.

We tried to develop a method allowing us to include more uncertainty terms in the analysis that previous studies using the inversion methodology described in Sections 2. The measurement error and the uncertainty in the determination of the equilibrium temperature profile have been included in previous studies (e.g., Beltrami et al., 2015a; Jaume-Santero et al., 2016; Pickler et al., 2016, 2018), but other sources of uncertainty remained unaddressed. The objective of the PPI method is to comprehensibly estimate the uncertainty due to as many factors affecting the inversion of the profiles as possible. To this end, we explore the range of reasonable thermal properties within borehole temperature profiles, as the thermal properties are typically unknown at most borehole locations. We also attempt to include the uncertainty related to the number of eigenvalues employed in the inversion, as there is no general rule to determine the total number of eigenvalues that should be conserved in the process.

Therefore, we are not trying to perform a bayesian inversion, we just generalize a typical inversion method to account for more sources of uncertainty than in previous studies using the evaluation of large ensembles of climate model simulations as inspiration (Knutti et al., 2017). Even more, our method is markedly different to a bayesian inversion, such as the one used in Shen and Beck, (1991) and Hopcroft et al., (2007). Nevertheless, it has been shown that all inversion methods retrieve similar surface signals from the same subsurface profiles (Shen et al., 1992).

A second comment is that I guess that sigma in equation 17 is also depth-dependent. If not, please state clearly. If yes, would it have an impact?

We indicated that sigma corresponds with the typical measurement error in borehole profiles, and therefore it is constant (line 248 of the original manuscript, line 259 on the new version of the manuscript). As stated in Knutti et al., (2017), the sigma parameter in Eq. 16 (Eq. 17 in the original manuscript) is just a value determining what RSMEs are

consider to be large or small. Therefore, the results will vary if changing sigma. Indeed, we could define a sigma that depends on depth, but we think that using a constant sigma improves the clarity of the method, as this is the first borehole study using it. A future study may evaluate the effect of this parameter on the retrieved inversions, but that is out of the scope of this work.

4) The main claim of the study is that the ground heat flux cannot be neglected. I miss a more direct comparison with the ocean heat flux, so that the reader gets a clearer idea. Probably, the ocean heat flux is much larger but the authors can more clearly elaborate their point.

We discussed the observed proportions of heat within the ocean and the continental subsurface in the Introduction of the original manuscript (lines 22-23 of the original manuscript). Nevertheless, we have included a comparison of the new estimates of ground heat flux at the surface presented in the manuscript with the ocean heat flux and the rest of terms of the Earth's heat inventory (lines 404-409).

Particular comments

5) line 30 'and sea level rise'. This is the major consequence of increase in ocean heat storage, so it is surprising that it is included with 'The rest of the components in the climate system'.

The reviewer is right, both ice melting and thermal expansion of the ocean contributes almost equally to sea level rise (Oppenheimer et al., 2019). We have changed the Introduction to clarify this point (lines 25-26 and 30-31).

6) line 63 'the model resolution for obtaining stable solutions'. the vertical resolution.

In fact, we were referring to the number of eigenvalues used to invert the borehole profile. We have clarified this on the new version of the manuscript (line 62).

7) line 75' These results also support previous estimates of temperature change since preindustrial times based on meteorological observations and CGCM simulations, using estimates from an independent source of data and considering the most distant period of time to determine preindustrial conditions to our knowledge. This paragraph is unclear and hard to read.

We have changed the last paragraph of the Introduction on the new version of the text (lines 74-80).

8) line 82 In borehole climatology, the continental subsurface is typically represented as a semi-infinite homogeneous half-space without internal sources of heat, where energy exchanges at the land surface and heat flux from the Earth's interior are considered as the'. Half-space is not a well-defined term. Please, rephrase this paragraph more clearly.

By half-space we meant a mathematical space from the surface to an infinite depth, as the radius of the Earth is long enough to be considered infinite in this problem. We have included a more detailed definition on the new version of the text (lines 83-86).

9) line 212 'the 95% confidence interval (two standard deviations) of the anomaly profile'. This is only (approximately) true if the distribution is gaussian.

Indeed, we are considering gaussian distribution of errors in the measurements since we are using a linear regression analysis. We have reworded the terms on the text in order to avoid any confusion (lines 223-225).

#####

Reviewer #2

Review of Cuerta-Valero et al Long-Term Global Ground Heat Flux and Continental Heat Storage from Geothermal Data.

This paper represents a useful update and expansion of a large body of work that uses borehole temperature measurements to estimate surface temperature changes and accumulation of heat in the upper few hundred metres of the Earth's crust, both associated with recent climate change. Advances in the paper include (a) the addition of additional borehole temperature data, and (b) a new approach to the inversion of the borehole data that produces better estimates of the uncertainties.

The introduction section is a particularly useful, comprehensive summary of work in this area with an extensive reference list. Figure 3a, the updated ground temperature history from 1580 CE to present with uncertainty estimates is very important. It is shown in comparison to previous ground temperature histories and the meteorological record back to ~1900 and should be widely used as a constraint in climate reconstructions. The authors perhaps should make a stronger point that Fig3a (and the analysis that results in Fig 3a) shows about 0.4K of warming from pre-industrial times to the start of the observational meteorological record around 1880.

The reviewers suggest an interesting result. We have included a comment on the Results section as indicated by the reviewer (lines 326-331).

And the total land surface warming to present time (Fig 3a) is close to 1.4K. In view of that number I don't understand the sentence in the conclusions that reads "The magnitude of the retrieved changes in ground surface temperature in this analysis supports the claim that the Earth's surface has warmed by 0.7 K since preindustrial times." Nor the sentence in the abstract that includes "land temperature changes of 1K... during the last part of the 20th century relative to preindustrial times." These statements should be consistent with each other and with Fig. 3a.

Regarding the estimate of global temperature change since preindustrial times, that value is obtained as explained in the Discussion section (lines 357-372 of the original manuscript, lines 386-402 of the new version of the manuscript). The estimate is based on averages of land temperature reconstructions using the three inversion methods discussed in this analysis and a factor to convert land temperature changes into global temperature changes. That is, we use the averaged results for each inversion model as indicated in Tables 1, S1 and S2 to estimate the change in land temperature relative to preindustrial conditions --in this case, the mean temperature between ~1300 CE and ~1700 CE (lines 360-363 of the original manuscript, lines 389-391 of the new version of the manuscript). Then, we calculate global (land and ocean) temperature change by scaling the change in land temperatures to account for the probable change in ocean temperatures, resulting in an increase in global temperature of around 0.7 K since preindustrial times (lines 365-372 of the original manuscript, lines 397-399 of the new version of the manuscript).

We have added some changes in the Discussion to improve the clarity of the text (lines 386-402).

Attention to the following details would improve the manuscript. 1. In Eqn 1, R is nota thermal depth which would have dimensions of length. It is in fact the thermal resistance with units $m^2 K/W$.

The reviewer is right, we have changed this on the new version of the text (line 94).

2. In section 3.1, the criteria for accepting a borehole temperature log of 1 measurement in the 15-100m depth range and at least 3 measurements in the 250-310 m depth range seems pretty loose. It would be good to know why such a fairly lax criteria was chosen and how many sites creep into the data set as a result.

Indeed, we included three criteria to select suitable borehole logs for our analysis: at least one temperature measurements between 15 m and 100 m to ensure the borehole profile recorded climate information near the logging year, at least one temperature measurement between 250 m and 310 m to ensure all temperature anomaly profiles include information about seven centuries before the logging date, and at least three temperature measurements between 200m and 300 m in order to perform a linear regression analysis.

We have changed the text in order to clearly explain why these criteria are applied and the number of logs excluded due to this filtering (lines 171 and 178-185).

3. It is a personal style, but I would prefer fewer acronyms. Are the following all necessary: GHC, BTP, GSTH, GHFH, PPI, RMSE, PPIT?

Indeed we used several acronyms to obtain a better flow in the original text. Furthermore, we have included additional acronyms in the new version of the manuscript to facilitate the interpretation of figures, responding the petition of the first reviewer. We have kept the acronyms that are more important to maintain the flow of the text, those necessary to understand the results, and those that are typical in scientific works, removing those that were superfluous. A new appendix (page 17) includes the remaining acronyms and their definition in order to improve the interpretation of results and the readability of the manuscript.

Overall this paper is a very useful contribution to the climate change literature.

Additional References

- Oppenheimer, M., B.C. Glavovic, J. Hinkel, R. van de Wal, A.K. Magnan, A. Abd-Elgawad, R. Cai, M. Cifuentes-Jara, R.M. DeConto, T. Ghosh, J. Hay, F. Isla, B. Marzeion, B. Meyssignac, and Z. Sebesvari (2019). Sea Level Rise and Implications for Low-Lying Islands, Coasts and Communities. In: IPCC Special Report on the Ocean and Cryosphere in a Changing Climate [H.-O. Pörtner, D.C. Roberts, V. Masson Delmotte, P. Zhai, M. Tignor, E. Poloczanska, K. Mintenbeck, A. Alegría, M. Nicolai, A. Okem, J. Petzold, B. Rama, N.M. Weyer (eds.)]. In press.
- Shen, P. Y., and Beck, A. E. (1991). Least squares inversion of borehole temperature measurements in functional space, *J. Geophys. Res.*, 96(B12), 19965-19979, doi:10.1029/91JB01883.

Long-Term Global Ground Heat Flux and Continental Heat Storage from Geothermal Data

Francisco José Cuesta-Valero^{1,2}, Almudena García-García^{1,2}, Hugo Beltrami^{1,3}, J. Fidel González-Rouco⁴, and Elena García-Bustamante⁵

¹Climate & Atmospheric Sciences Institute, St. Francis Xavier University, Antigonish, NS, Canada.

²Environmental Sciences Program, Memorial University of Newfoundland, St. John's, NL, Canada.

³Department of Earth Sciences, St. Francis Xavier University, Antigonish, Nova Scotia, Canada.

⁴Universidad Complutense de Madrid, 28040 Madrid, Spain.

⁵Centro de Investigaciones Energéticas, Medioambientales y Tecnológicas (CIEMAT), 28040 Madrid, Spain.

Correspondence: Hugo Beltrami (hugo@stfx.ca)

Abstract. Energy exchanges among climate subsystems are of critical importance to determine the climate sensitivity of the Earth's system to greenhouse gases, to quantify the magnitude and evolution of the Earth's energy imbalance, and to project the evolution of future climate. Thus, ascertaining the magnitude and change of the Earth's energy partition within climate subsystems has become urgent in recent years. Here, we provide new global estimates of changes in ground surface temperature, ground surface heat flux and continental heat storage derived from geothermal data using an expanded database and new techniques. Results reveal markedly higher changes in ground heat flux and heat storage within the continental subsurface than previously reported, with land temperature changes of 1 K and continental heat gains of around 12 ZJ during the last part of the 20th century relative to preindustrial times. Half of the heat gain by the continental subsurface since 1960 have occurred in the last twenty years.

10 1 Introduction

Climate change is consequence of the current radiative imbalance at top-of-the-atmosphere, which delivers an excess amount of energy to the Earth's system in comparison with preindustrial conditions (Hansen et al., 2011; Stephens et al., 2012; Lembo et al., 2019). Nonetheless, the energy imbalance presents an interhemispheric asymmetry, being larger in the southern hemisphere (Loeb et al., 2016; Irving et al., 2019). This asymmetry causes an increase in the heat uptake by the ocean surface in the southern hemisphere in comparison with the ocean heat uptake in the northern hemisphere. Hence, a cross-equatorial northward transport of heat emerges to compensate this asymmetry (Lembo et al., 2019), in addition to the the global meridional heat transport caused by the different radiation levels reaching the tropical and polar oceans (Trenberth et al., 2019). The hemispheric distribution of heat uptake, heat storage and heat transport is expected to change under different emission scenarios (Irving et al., 2019), meaning that characterizing where the heat enters the system (uptake), where the heat is allocated (storage), and where the heat is redistributed (transport), is of critical importance to understand the evolution of climate change.

The vast majority of excess heat due to the Earth's energy imbalance is stored in the ocean (84-93%), followed by the cryosphere (4-7%) and the continental subsurface (2-5%), with the atmosphere showing the smaller heat storage term (1-4%) (Levitus et al., 2005; Church et al., 2011). Therefore, extensive resources are devoted to monitor and understand the evolution of the ocean heat content, since it is also an indirect method to study the magnitude and variations of the energy imbalance at top-of-atmosphere [\[..¹\]](#) and contributes to sea level rise (Palmer et al., 2011; Palmer and McNeall, 2014; Johnson et al., 2016; Riser et al., 2016; von Schuckmann et al., 2016; Oppenheimer et al., 2019). The rest of the components of the climate system have relevant roles in the Earth [\[..²\]](#) heat inventory, despite their small contribution to storage (Levitus et al., 2005; Church et al., 2011; Hansen et al., 2011; von Schuckmann et al., 2016). For instance, some energy-dependent processes are permafrost stability and the associated permafrost carbon feedback (MacDougall et al., 2012; Hicks Pries et al., 2017), changes in circulation patterns (Tomas et al., 2016; Screen et al., 2018) and sea level rise [\[..³\]](#) from ice melting (Jacob et al., 2012; Vaughan et al., 2013; Dutton et al., 2015; Oppenheimer et al., 2019). The additional energy in the atmosphere, cryosphere and continental subsurface also affects near-surface conditions, having important consequences for society. Increases in atmospheric heat content produce warmer surface air temperature and larger amounts of water content within the atmosphere that can impact crop yields, and consequently global food security (Lloyd et al., 2011; Rosenzweig et al., 2014; Phalkey et al., 2015; Campbell et al., 2016) as well as degrading human health due to heat stress (Sherwood and Huber, 2010; Matthews et al., 2017; Watts et al., 2019). Floods induced by extreme precipitation events, which frequency and intensity are affected by the amount of water in the atmosphere, as well as floods induced by sea level rise caused by the thermal expansion of the ocean and melting of Greenland and Antarctica ice sheets, are likely to impact human settlements (McGranahan et al., 2007; Kundzewicz et al., 2014). Furthermore, all these alterations of surface environmental conditions may enhance the spread of diseases (Levy et al., 2016; McPherson et al., 2017; Wu et al., 2016; Watts et al., 2019), among other potential risks.

Long-term global estimates of heat storage within the continental subsurface [\[..⁴\]](#) have been previously estimated from borehole temperature profile (BTP) measurements. Changes in the energy balance at the land surface add or remove heat from the upper continental crust, changing the long-term subsurface equilibrium temperature profile (Beltrami, 2002b). Such temperature changes propagate through the ground by conduction, and are recorded in the subsurface as perturbations on the quasi-steady state vertical temperature profile. Borehole climatology consists in estimating variations in ground surface temperature and heat flux from these recorded alterations in the subsurface thermal regime. Ground [\[..⁵\]](#) surface temperature histories and ground heat flux histories have been retrieved from BTP measurements both at regional and at hemispheric scales for multi-century to multi-millennial time periods (Lane, 1923; Cermak, 1971; Beck, 1977; Vasseur et al., 1983; Lachenbruch and Marshall, 1986; Huang et al., 2000; Harris and Chapman, 2001; Roy et al., 2002; Beltrami and Bourlon, 2004; Hartmann and Rath, 2005; Beltrami et al., 2006; Hopcroft et al., 2007; Chouinard and Mareschal, 2009; Davis et al., 2010; Barkaoui et al., 2013; Demezhko and Gornostaeva, 2015; Jaume-Santero et al., 2016; Pickler et al., 2016), constituting an useful reference

¹removed: (Palmer et al., 2011; Palmer and McNeall, 2014; Johnson et al., 2016; Riser et al., 2016; von Schuckmann et al., 2016)

²removed: 's energy budget

³removed: (Jacob et al., 2012; Vaughan et al., 2013; Dutton et al., 2015)

⁴removed: (ground heat content, GHC)

⁵removed: Surface Temperature Histories (GSTHs) and Ground Heat Flux Histories (GHFHs)

for evaluating climate simulations performed by [⁶]atmosphere-ocean coupled general circulation models beyond the observational period (González-Rouco et al., 2009; Stevens et al., 2008; MacDougall et al., 2010; Cuesta-Valero et al., 2016; García-García et al., 2016; Cuesta-Valero et al., 2019), as well as for evaluating reconstructions derived from other paleoclimate data (Fernández-Donado et al., 2013; Masson-Delmotte et al., 2013; Jaume-Santero et al., 2016; Beltrami et al., 2017).

Previous global estimates of GHC, [⁷]ground heat flux histories and ground heat temperature histories have been retrieved from BTP measurements nearly two decades ago (Pollack et al., 1998; Huang et al., 2000; Beltrami et al., 2002; Beltrami, 2002a; Pollack and Smerdon, 2004), including a limited characterization of uncertainties. Meanwhile, advances in borehole methodology have allowed to assess the uncertainty in borehole reconstructions induced by a series of factors: the presence of advection and freezing phenomena, the sampling rate and the depth range used in the determination of the quasi-equilibrium profile, the depth of the log, the different logging dates of the profiles, the noise in the measured profile, the [⁸]number of retained eigenvalues for obtaining stable solutions, the spatial distribution of borehole measurements, and the transient variations in the subsurface thermal regime due to the end of the last glacial cycle (Bodri and Cermak, 2005; Hartmann and Rath, 2005; Reiter, 2005; González-Rouco et al., 2006; Mottaghy and Rath, 2006; González-Rouco et al., 2009; Rath et al., 2012; Beltrami et al., 2015a, b; García-García et al., 2016; Jaume-Santero et al., 2016; Beltrami et al., 2017; Melo-Aguilar et al., 2019). These advances together with the availability of new BTP measurements make necessary an update of the global long-term evolution of ground heat content from borehole data.

Here, we use an expanded borehole database to estimate global [⁹]ground surface temperature histories, ground heat flux histories, and ground heat content within the continental subsurface for the last four centuries. Surface temperature and heat flux histories are retrieved from each BTP using a Singular Value Decomposition (SVD) algorithm, one of the standard borehole methodologies employed in previous analyses (Beltrami et al., 2002; Beltrami, 2002a), as well as a new approach based on generating an ensemble of inversions for each temperature profile to explore additional sources of uncertainty unaddressed in previous global borehole reconstructions.

We find higher values of surface temperature, ground heat flux at the surface and ground heat content from borehole data than previously reported. [¹⁰]The estimated global surface temperature change since preindustrial times is in agreement with meteorological observations, proxy reconstructions and general circulation model simulations. The higher continental heat storage implies that a larger amount of the additional energy gained by the Earth system is allocated within the continental subsurface than previously thought [¹¹]. These results reinforce the necessity of monitoring the continental heat storage and

⁶removed: Coupled General Circulation Models (CGCMs)

⁷removed: GHFHs and GSTHs

⁸removed: model resolution

⁹removed: GSTHs, GHFHs, and GHC

¹⁰removed: These results imply

¹¹removed: , reinforcing

the need for improving the representation of the land component of the [\[..¹² \]Earth's heat inventory](#) within long-term climate
80 simulations. [\[..¹³ \]](#)

2 Theory

2.1 Subsurface Temperature Profile

In borehole climatology, the continental subsurface is typically represented as a semi-infinite [\[..¹⁴ \]solid bounded by the plane](#)
 [\$z = 0\$ and extend to infinity in the direction of \$z\$ positive \(i.e., downwards, Carslaw and Jaeger, 1959\). That is, the subsur-](#)
85 [face is considered as an homogeneous medium of infinite depth](#) without internal sources of heat, where energy exchanges at
the land surface and heat flux from the Earth's interior are considered as the upper and bottom boundary conditions. The local
subsurface thermal regime is, therefore, the result of a balance between the surface thermal state and the thermal conditions
of the Earth's interior. If surface conditions remain stable at long time scales, the subsurface thermal regime would be at a
quasi-equilibrium since the flux from the Earth's interior is constant at geological time scales (million years). Thereby, the
90 subsurface temperature profile can be expressed as the superposition of the transient temperature due to changes in the surface
conditions (T_t) relative to the long-term quasi-equilibrium state (Carslaw and Jaeger, 1959):

$$T(z) = T_0 + q_0 R(z) + T_t(z), \quad (1)$$

where z is depth, T_0 is the long-term surface temperature, q_0 is the heat flux from the Earth's interior, and $R(z) = \int_0^z \frac{dz'}{\lambda(z')}$
is the thermal [\[..¹⁵ \]resistance \(in \$\text{m}^2 \text{K W}^{-1}\$ \)](#), which depends on the thermal conductivity (λ) of the ground (Bullard and
95 Schonland, 1939). Since measurements of thermal conductivity profiles are scarce and the measured profiles typically display
variations around a constant value with depth, the thermal conductivity can be assumed to be constant and Equation 1 can be
rewritten as

$$T(z) = T_0 + \Gamma \cdot z + T_t(z), \quad (2)$$

with $\Gamma = \frac{q_0}{\lambda}$ the equilibrium subsurface thermal gradient. The term $T_0 + \Gamma \cdot z$ in Equation 2 describes the quasi-equilibrium
100 temperature profile, and can be determined from the deepest part of a BTP - that is, the least affected part of the log by recent
perturbations of the energy balance at the surface.

The propagation of temperature variations in a one-dimensional, homogenous, isotropic medium without internal sources of
heat is governed by the heat diffusion equation

$$\frac{\partial T}{\partial t} = \kappa \frac{\partial^2 T}{\partial z^2}, \quad (3)$$

¹²removed: energy budget

¹³removed: These results also support previous estimates of temperature change since preindustrial times based on meteorological observations and CGCM
simulations, using estimates from an independent source of data and considering the most distant period of time to determine preindustrial conditions to our
knowledge.

¹⁴removed: homogenous half-space

¹⁵removed: depth

105 where T is temperature, t is time, κ is the thermal diffusivity of the medium and z is the spatial dimension. An instantaneous change in surface temperature (ΔT_0) is propagated through the ground as described in Equation 3, altering the quasi-equilibrium temperature profile with time following (Carslaw and Jaeger, 1959)

$$T(z, t) = \Delta T_0 \cdot \operatorname{erfc} \left(\frac{z}{2\sqrt{\kappa t}} \right), \quad (4)$$

where erfc is the complementary error function, and t is time since the surface temperature change. A series of surface temperature perturbations will propagate through the ground as the superposition of transient variations of the long-term subsurface thermal regime:

$$T_t(z) = \sum_{i=1}^N \Delta T_i \left[\operatorname{erfc} \left(\frac{z}{2\sqrt{\kappa t_i}} \right) - \operatorname{erfc} \left(\frac{z}{2\sqrt{\kappa t_{i-1}}} \right) \right], \quad (5)$$

where ΔT_i are changes in surface temperature at i time step. Equation 5 is also the solution of the forward problem: given an upper (surface) boundary condition, this equation describes the perturbation of the subsurface temperature profile in response to a temporal series of ground surface temperature changes (Lesperance et al., 2010).

2.2 Subsurface Flux Profile

Since the conductive heat flux (q) in an isotropic medium is related to the temperature gradient of the subsurface temperature profile by Fourier's equation

$$q = -\lambda \frac{\partial T}{\partial z}, \quad (6)$$

120 the propagation of heat flux through a one-dimensional, homogenous medium without internal sources of heat satisfies:

$$\frac{\partial q}{\partial t} = \kappa \frac{\partial^2 q}{\partial z^2}. \quad (7)$$

That is, the propagation of both temperature and heat flux through the ground is governed by the diffusion equation (Carslaw and Jaeger, 1959; Turcotte and Schubert, 2002). As in the case of temperature profiles, the heat flux profile can be expressed as

$$125 \quad q(z) = q_0 + q_t(z), \quad (8)$$

where q_0 is the equilibrium geothermal flux from the Earth's interior. Therefore, alterations in the subsurface equilibrium flux profile due to an instantaneous perturbation of the long-term surface flux (Δq_0) can be expressed as

$$q(z, t) = \Delta q_0 \cdot \operatorname{erfc} \left(\frac{z}{2\sqrt{\kappa t}} \right), \quad (9)$$

where t is time since the perturbation. A series of perturbations of the surface flux generates a superposition of transient variations of the long-term subsurface thermal gradient as

$$130 \quad q_t(z) = \sum_{i=1}^N \Delta q_i \left[\operatorname{erfc} \left(\frac{z}{2\sqrt{\kappa t_i}} \right) - \operatorname{erfc} \left(\frac{z}{2\sqrt{\kappa t_{i-1}}} \right) \right], \quad (10)$$

mirroring the forward model for surface temperature variations described in Equation 5 and representing the solution of the forward problem for variations in surface heat flux (Beltrami, 2001; Beltrami et al., 2006).

2.3 Inversion Problem

- 135 The inversion problem consists in retrieving the past ground surface temperature histories that generated the observed temperature perturbation profiles, or the ground heat flux histories that generated the heat flux anomaly profiles. A system of equations can be derived by combining Equations 2 and 5 for the temperature case, and Equations 8 and 10 for the heat flux case, with the solution of such systems yielding an estimate of the past long-term evolution of surface temperature and surface heat flux, respectively (Vasseur et al., 1983; Beltrami et al., 1992; Mareschal and Beltrami, 1992; Shen et al., 1992; Beltrami, 2001; 140 Hartmann and Rath, 2005). [..¹⁶]The system can be expressed [..¹⁷]as a matrix equation of the form:

$$\mathbf{T}_{obs} = \mathbf{M}\mathbf{T}_{model}, \quad (11)$$

[..¹⁸]where \mathbf{T}_{obs} is the data vector (anomaly temperature profile of heat flux profile), \mathbf{M} is the matrix containing the coefficients of the system, and \mathbf{T}_{model} is a vector containing the step change [..¹⁹]model to be determined [..²⁰]. The elements [..²¹]of \mathbf{M} are defined from the forward model for temperature (Equation 5):

$$145 \quad M_{i,j} = \operatorname{erfc}\left(\frac{z_i}{2\sqrt{\kappa t_j}}\right) - \operatorname{erfc}\left(\frac{z_i}{2\sqrt{\kappa t_{j-1}}}\right) [..²²], \quad (12)$$

- [..²³]and a similar system can be written in terms of heat flux using Equation 10. The rank of the system is given by the number of time steps in the proposed inversion model (N_t), and is generally smaller than the number of measurements in the profile (N_z). That is, there are more equations than parameters in the system, thus both the temperature and heat flux systems are overdetermined. Therefore, these systems are solved using a Singular Value Decomposition algorithm (Lanczos, 1961) as 150 the one described in Mareschal and Beltrami (1992) and Clauser and Mareschal (1995).

[..²⁴]

[..²⁵]

[..²⁶]This SVD algorithm decomposes the matrix of coefficients as

$$\mathbf{M} = \mathbf{U}\mathbf{S}\mathbf{V}^T, \quad (13)$$

¹⁶removed: This

¹⁷removed: for the temperature case as

¹⁸removed: where $T_t(z_i)$ are the temperature anomalies at the depth z_i , and ΔT_i are

¹⁹removed: in surface temperature

²⁰removed: , that is the proposed inversion model

²¹removed: $M_{i,j}$

²³removed: Note that

²⁴removed: The system in Equation ?? can be expressed as a matrix equation of the form:

²⁶removed: where \mathbf{T}_{obs} is the data vector (anomaly temperature profile of heat flux profile), \mathbf{M} is the matrix containing the coefficients given by Equation 12 (or the equivalent expression for the case of heat flux), and \mathbf{T}_{model} is a vector containing the step change model to be determined. The

155 with \mathbf{U} and \mathbf{V} orthonormal matrices of dimension $N_z \times N_z$ and $N_t \times N_t$, respectively, and \mathbf{S} a rectangular matrix ($N_z \times N_t$) containing the eigenvalues α_j in the diagonal. Therefore, the general solution can be expressed as:

$$\mathbf{T}_{model} = \mathbf{M}^{-1}\mathbf{T}_{obs} = \mathbf{V}\mathbf{S}^{-1}\mathbf{U}^T\mathbf{T}_{obs}. \quad (14)$$

160 However, the solution of Equation 14 is dominated by noise from small eigenvalues, as the only non-zero elements of \mathbf{S}^{-1} are the inverse of the eigenvalues in the diagonal of the matrix (Mareschal and Beltrami, 1992). Accordingly, small eigenvalues need to be removed from \mathbf{S}^{-1} (i.e., are replaced by zeros) for stabilizing the solution, but at the cost of losing temporal resolution in the model.

3 Analysis

3.1 Borehole Data

165 Borehole Temperature Profiles (BTPs) were collected from four databases. The National Oceanic and Atmospheric Administration (NOAA) server (NOAA, 2019) contains global data; the database presented in Jaume-Santero et al. (2016) includes data for North America; logs from Tasmania were retrieved from Suman et al. (2017); and measurements from Chile were obtained from Pickler et al. (2018). Profiles from all databases were screened to avoid repetitions, resulting in 1266 independent logs in total.

170 Nonetheless, not all these BTPs are employed in the analysis. A process for selecting suitable logs is applied, based on trimming the maximum depth of the available BTPs and requiring a certain number of measurements at critical depth ranges. [..²⁷] Three profiles containing less than three measurements between 200 m and 300 m were discarded, since it was impossible to perform a linear regression analysis to determine the quasi-equilibrium profile (see Section 3.3 below). All remaining logs were truncated from 15 m to 300 m depth[..²⁸]. Thereby, we ensure that the profiles include information from the logging year to several centuries back in time and cover the same time span, since the relationship between time (t) required for a change in 175 the surface energy balance to reach a certain depth (z) can be approximated as (Carslaw and Jaeger, 1959; Pickler et al., 2016; Cuesta-Valero et al., 2019):

$$t \approx \frac{z^2}{4\kappa}, \quad (15)$$

180 [..²⁹] Furthermore, at least a temperature measurement between 15 m and 100 m is required, since this depth range approximately corresponds to a temporal period of 50yr before the logging date, depending on the considered diffusivity, κ , in Equation 15. This period is the largest step change used to retrieve surface histories in this analysis (Section 3.3), thus it is highly desirable a measurement in this depth range. Following the same reasoning, another temperature

²⁷removed: Thereby, all BTPs used here must include at least one temperature measurement between 15 m and 100 m, and between 250 m and 310 m.

Profiles

²⁸removed: , resulting in 1079 logs selected for this analysis

²⁹removed: This depth filtering

measurement between 250 m and 310 m is requested in order to ensure that the inversions include information about approximately four centuries before the logging date (Equation 15). As result of applying these two criteria to the global network of borehole measurements 184 logs were excluded from the analysis, with 1079 BTPs deemed suitable for our analysis.

The depth filtering explained above constitutes the main methodological difference in comparison with previous borehole studies [..³⁰][..³¹][..³²][..³³](including Beltrami et al., 2002; Beltrami, 2002a), since those assessments analyzed all available logs independently of their depth range, thus mixing temporal references. However, recent works have shown that using subsurface profiles with different depths affects the estimated [..³⁴]ground surface temperature histories (González-Rouco et al., 2009; Beltrami et al., 2015b; Melo-Aguilar et al., 2019). This issue is avoided here by the selection criteria applied to the assembled BTP database. Additionally, BTPs were measured at different dates, but the logging year of the profiles had been taken into account only in a small number of works (e.g., González-Rouco et al., 2009; Jaume-Santero et al., 2016; Melo-Aguilar et al., 2019). We aggregate the retrieved [..³⁵]ground surface temperature histories and ground heat flux histories from BTPs considering the logging date of each borehole profile (Figure 1), thus the number of borehole inversions available for analysis varies with time.

3.2 Surface Air Temperature Data

Meteorological measurements of Surface Air Temperature (SAT) from the Climate Research Unit (CRU) at East Anglia university (named SAT_CRU hereinafter) are also used in this study to compare with borehole estimates. Mean global SAT anomalies relative to 1961-1990 Common Era (CE) from the CRU TS 4.01 product (Harris et al., 2014) are employed to compare with [..³⁶]ground surface temperature histories retrieved from borehole profiles. Results for the entire CRU spatial and temporal domains are provided from 1901 CE to 2016 CE, as well as results considering only locations and dates containing borehole inversions.

3.3 Inversion of Borehole [..³⁷]Profiles

3.3.1 Standard Inversions

We invert the same truncated BTPs to obtain [..³⁸]ground surface temperature histories considering the uncertainty from the determination of the equilibrium profile, as a reference to compare with the uncertainty estimates of recent works using the same SVD algorithm (Beltrami et al., 2015a; Jaume-Santero et al., 2016; Pickler et al., 2016, 2018). In this case, all logs are inverted

³⁰removed: (?),

³¹removed: including

³²removed: beltrami2002continental, beltrami2002climate

³³removed: ,

³⁴removed: GSTHs

³⁵removed: GSTHs and GHFHs

³⁶removed: GSTHs

³⁷removed: Temperature

³⁸removed: GSTHs

considering a model based on a thermal conductivity of $3 \text{ W m}^{-1} \text{ K}^{-1}$, a volumetric heat capacity of $3 \times 10^6 \text{ J m}^{-3} \text{ K}^{-1}$, and thus a thermal diffusion of $1 \times 10^{-6} \text{ m}^2 \text{ s}^{-1}$. The same SVD algorithm used in Beltrami (2002a) and Beltrami et al. (2002) is applied to generate the [\[..³⁹ \]ground surface temperature histories](#) for three step change models, since there is no preferential inversion model. All BTPs are inverted using models based on step changes of 25, 40 and 50 years to reconstruct the surface signal for 400 years before the logging date of the profile (i.e., inversion models of 16, 10 and 8 time steps, respectively), with all inversions including the four highest eigenvalues. We regard these as the [\[..⁴⁰ \]GST_Standard ensemble](#) and will serve as a reference to the methods described in Section [\[..⁴¹ \]3.3.2](#).

The equilibrium temperature profile is estimated in order to obtain the anomaly profile that is inverted by the SVD algorithm. The equilibrium profile is estimated from the deepest part of each truncated BTP, since that is the zone least affected by the recent climate change signal (grey zone in Figure 2a). A linear regression analysis of the lowermost 100 m of each profile (from 200 m to 300 m depth in our analysis, straight lines in Figure 2a) is performed to estimate the values determining the quasi-equilibrium temperature profile, that is, the long-term surface temperature (T_0) and the equilibrium geothermal gradient (Γ). We use the last hundred meters and not a longer depth range to reach a balance between the characterization of noise and retrieving as much climatic information as possible from each log (Beltrami et al., 2015a). The anomaly profile is then retrieved by subtracting the quasi-equilibrium temperature profile from the measured log (black dots in Figure 2b). Additionally, the [\[..⁴² \]errors](#) in the slope (Γ) and intercept (T_0) [\[..⁴³ \]](#)allow to obtain two extremal temperature anomaly profiles [\[..⁴⁴ \]](#)(red and blue dots in Figure 2b). The inversion of these additional anomaly profiles [\[..⁴⁵ \]is considered as the error in the retrieved ground surface temperature histories](#) from each borehole. We do not invert the heat flux profiles using this approach, but provide surface flux estimates from the retrieved surface temperature histories to compare with Beltrami (2002a) and Beltrami et al. (2002) (see Section 3.4 for details).

3.3.2 Perturbed Parameter Inversions of Temperature Profiles

Although the inversion approach used in previous studies was successful in retrieving the past long-term evolution of ground surface temperatures and ground heat fluxes at BTP locations, several sources of uncertainty remained unaddressed. Here, we use a new approach based on generating an ensemble of inversions using the SVD algorithm described in Mareschal and Beltrami (1992) for each borehole profile to account for as many sources of uncertainty as possible. The ensemble contains inversions retrieved by considering a range of values for the thermal properties, different number of eigenvalues in the SVD algorithm, as well as the inversions of the two additional anomaly profiles generated from the estimate of the quasi-equilibrium temperature profile. Thereby, three sources of uncertainty are considered in the analysis, expanding the methodology of previous studies based on BTP inversions performed with the same SVD algorithm (Beltrami et al., 2015a; Jaume-Santero et al.,

³⁹removed: GSTHs

⁴⁰removed: Standard inversion approach

⁴¹removed: ??

⁴²removed: uncertainties

⁴³removed: values

⁴⁴removed: representing the 95% confidence interval (two standard deviations) of the anomaly profile (

⁴⁵removed: provide the 95% confidence interval of the retrieved GSTHs

2016; Pickler et al., 2016, 2018). Additionally, all BTPs are inverted using the three different inversion models used in the Standard approach. We name this new approach as the Perturbed Parameter Inversion (PPI thereafter) due to the similarities with the generation of perturbed parameter ensembles in climate modeling (e.g., Collins et al., 2011).

240 The PPI approach considers the three anomaly profiles estimated from the uncertainty in determining the subsurface equilibrium profile as in the Standard approach (e.g., Jaume-Santero et al., 2016, and section above). Each of these anomaly profiles is inverted using different values of thermal conductivity (λ) and volumetric heat capacity (ρC). The values of thermal conductivity considered in this analysis are 2.5, 3 and $3.5 \text{ W m}^{-1} \text{ K}^{-1}$, while the values for volumetric heat capacity are 2.5, 3 and $3.5 \times 10^6 \text{ J m}^{-3} \text{ K}^{-1}$. That is, the typical values of $3 \text{ W m}^{-1} \text{ K}^{-1}$ and $3 \times 10^6 \text{ J m}^{-3} \text{ K}^{-1}$ for the conductivity and heat
 245 capacity, respectively, as well as two extremal cases to account for plausible variations of thermal properties. The combination of each pair of conductivities and heat capacities yields a series of 9 values for thermal diffusivity ranging between 0.7 and $1.4 \times 10^{-6} \text{ m}^2 \text{ s}^{-1}$. Additionally, estimates obtained for the three inversion models use different numbers of eigenvalues to retrieve the surface signal, attending to the sensitivity of the SVD algorithm to small eigenvalues and to the length of each time step in the inversion model (Hartmann and Rath, 2005; Melo-Aguilar et al., 2019). Thus, inversions based on the 25 yr step
 250 change model use the highest 3, 4 and 5 eigenvalues, inversions based on the 40 yr step change model use the highest 2, 3 and 4 eigenvalues, and inversions based on the 50 yr step change model use the highest 2, 3 and 4 eigenvalues.

Therefore, the PPI ensemble generated from each original borehole temperature profile consists of 243 different [\[..⁴⁶\]](#) [surface temperature inversions](#). All these inversions are then propagated using a purely conductive forward model in order to obtain synthetic BTPs as described in Equation 5, which are compared with the original anomaly profiles (Figure 2c). This allows to
 255 evaluate the performance of the different parameter variants in the inversion and to attribute relative weights to them. Root mean squared errors (RMSEs) between the anomaly profiles and the synthetic profiles generated from the inversions are computed to assign a weight to each inversion following a gaussian function as in Knutti et al. (2017):

$$w_i = \exp \left\{ \frac{-\text{RMSE}_i^2}{\sigma^2} \right\}, \quad (16)$$

where w_i is the weight associated to the i th inversion, and σ is a parameter determining which RMSEs are deemed as large and
 260 which are deemed as small. We select the typical error in BTP measurements ($\sigma = 50 \text{ mK}$) as criterium to assess how each inversion should be weighted, that is, to evaluate which RSMEs are large and which are small.

Thus, each inversion is classified according to the realism of its associated synthetic anomaly profile. Nevertheless, unrealistic solutions may arise as result of the broad range of parameters and inversion models considered even after weighting each inversion. Hence, we introduce here a new additional criterium to asses all the 243 inversions per BTP based on the variability
 265 of surface air temperature measurements as a guide. A temperature change in an inverted [\[..⁴⁷\]](#) [ground surface temperature history](#) is considered unrealistic if it is larger than the maximum change obtained from the histogram of temperature variations between consecutive time steps from the SAT_CRU data. This histogram is created by aggregating temperature changes between consecutive time steps after averaging the original temperature series at each grid cell in temporal windows of 25

⁴⁶removed: GSTH inversions(see the case for GHFHs below)

⁴⁷removed: GSTH

years (i.e., running means of 25 years, Figure S1). The averaging of the original temperature series is necessary to remove
 270 high-frequency variability that is not present in [..⁴⁸]ground surface temperature histories from BTP inversions. That is, a
 [..⁴⁹]ground surface temperature history is deemed as unrealistic and removed from the analysis if the temperature change
 between at least one pair of consecutive time steps is larger than 2.57 K for the three inversion models. The 5th, 50th, and 95th
 weighted percentiles are eventually estimated from the ensemble of remaining inversions (Figure 2d) for each borehole profile.
 The ensemble containing the weighted percentiles from [..⁵⁰]ground surface temperature histories from all BTPs is called
 275 GST_PPIT ensemble hereinafter.

3.3.3 Perturbed Parameter Inversions of Heat Flux Profiles

The same approach is applied to the corresponding heat flux profiles to retrieve ground heat flux histories from borehole data.
 The heat flux profiles are generated from the three estimated temperature anomaly profiles for each measured log using the
 Fourier's equation (Equation 6) as

$$280 \quad q_i = -\lambda \frac{T_{i+1} - T_i}{z_{i+1} - z_i}. \quad (17)$$

Those profiles are then inverted using the PPI approach described above. [..⁵¹]That is, an ensemble of inversions is generated
 using the same SVD algorithm, the same range of thermal properties, and the same number of eigenvalues as for the
 GST_PPIT ensemble of Section 3.3.2. Thus, the thermal conductivity for estimating the heat flux profile (λ in Equation
 17) is set to match the values used for each perturbed parameter inversion. Thereby, we obtain 243 heat flux histories for each
 285 original log, which are compared to the corresponding flux anomaly profile (using Equation 10) and weighted as in the case
 of temperature histories (Equation 16). Changes in [..⁵²]ground heat flux histories are compared to the histogram created by
 aggregating heat flux changes estimated from the CRU temperature data and Equation 18 (GHF_CRU hereinafter) in order to
 discard unrealistic heat flux histories. As in the case of temperature changes, heat flux changes between consecutive time steps
 are aggregated after averaging the original heat flux series from each grid cell over temporal windows of 25 years (Figure S1).
 290 Surface heat flux histories are deemed unrealistic if the difference between at least one pair of consecutive time steps is larger
 than 0.51 W m^{-2} for the three inversion models. The ensemble containing the 5th, 50th and 95th weighted percentiles from
 [..⁵³]ground heat flux histories from all BTPs is called GHF_PPIF ensemble hereinafter.

Estimates from temperature profiles and from heat flux profiles using the PPI and Standard approaches need to include
 inversions from the same number of BTPs to obtain the same geographical representation of surface temperature and heat flux
 295 changes. This requirement reduces the number of borehole considered in the analysis to 1060, 1072 and 1074 for the 25 yr, 40

⁴⁸removed: GSTHS

⁴⁹removed: GSTH

⁵⁰removed: GSTHS

⁵¹removed: The thermal

⁵²removed: GHFHs

⁵³removed: GHFHs

yr and 50 yr inversion models, respectively, since not all BTPs provide with [\[.54\]](#) ground surface temperature histories and ground heat flux histories complying with all criteria explained in [\[.55\]](#) Sections 3.3.2 and 3.3.3, respectively.

3.4 Flux Estimates from Surface Temperatures

The relationship between surface flux (q) and a temporal series of surface temperatures can be expressed as (Wang and Bras, 1999; Beltrami, 2001)

$$q_{t_N} = \frac{2\lambda}{\sqrt{\pi\kappa\Delta t}} \sum_{i=1}^{N-1} \left\{ (T_i - T_{i+1}) \left(\sqrt{N-i} - \sqrt{N-i-1} \right) \right\}, \quad (18)$$

where Δt is the length of the time steps and T_i is surface temperature at the i th time step. We estimate ground heat flux histories at the surface from [\[.56\]](#) ground surface temperature histories retrieved from both the Standard (GHF_Standard ensemble) and PPI approaches (GHF_PPIT ensemble). Thermal properties for estimating heat fluxes from [\[.57\]](#) ground surface temperature histories obtained with the Standard inversion approach are set to $\lambda = 3 \text{ W m}^{-1} \text{ K}^{-1}$ and $\kappa = 1 \times 10^{-6} \text{ m}^2 \text{ s}^{-1}$, while thermal properties for estimating heat fluxes from [\[.58\]](#) ground surface temperature histories included in the GST_PPIT ensemble are set as those associated to the corresponding individual [\[.59\]](#) ground surface temperature history. Heat flux estimates are also provided using Equation 18 and SAT_CRU temperature data [\[.60\]](#) (GHF_CRU ensemble mentioned in Section 3.3.3) in order to create the histogram of heat flux changes displayed in Figure S1, considering the same thermal properties as in heat flux estimates from [\[.61\]](#) ground surface temperature histories retrieved by the Standard approach.

4 Results

Ground surface temperature histories estimated using a 25 yr inversion model together with the Standard approach and the new GST_PPIT ensemble show temperature increases that are particularly large during the second half of the 20th century in comparison with preindustrial conditions (Figure 3a). This is in agreement with meteorological observations of surface air temperatures (red and orange lines in the mentioned figure), as well as with previous studies using both borehole temperature profiles and proxy data (Pollack et al., 1998; Huang et al., 2000; Beltrami, 2002a; Pollack and Smerdon, 2004; Fernández-Donado et al., 2013; Masson-Delmotte et al., 2013). Both approaches used to retrieve [\[.62\]](#) ground surface temperature histories from temperature profiles display a remarkable agreement during the whole period, as well as similar temperature changes to those shown by [\[.63\]](#) SAT_CRU temperatures for the observational period. Global mean temperature changes

⁵⁴removed: GSTHs and GHFHs

⁵⁵removed: Section ??

⁵⁶removed: GSTHs

⁵⁷removed: GSTHs

⁵⁸removed: GSTHs

⁵⁹removed: GSTH

⁶⁰removed: in

⁶¹removed: GSTHs

⁶²removed: GSTHs

⁶³removed: CRU surface

320 between 1950-1975 CE and 1975-2000 CE reach 0.3 K for the [GST_PPIT](#) ensemble and 0.4 K for the [\[..⁶⁴ \]GST_Standard ensemble](#) (Table 1), with mean temperature changes from [SAT_CRU](#) data yielding approximately 0.4 K using both the entire dataset and locations and dates containing BTP inversions. [\[..⁶⁵ \]](#)

[Ground surface temperature histories](#) present slightly higher temperature changes since preindustrial times than previously reported, with results ranging from 1.0 ± 0.1 K to 1.2 ± 0.2 K for the last part of the 20th century considering results from the three inversion models (Tables 1, S1 and S2) in comparison to the ~ 0.9 K reported in previous works (Huang et al., 2000; Harris and Chapman, 2001; Beltrami, 2002a; Pollack and Smerdon, 2004). Furthermore, [ground surface temperature histories show a temperature increase of around \$0.5 \pm 0.3\$ K using the \[GST_Standard ensemble\]\(#\) and \$0.3 \pm 0.5\$ K using the \[GST_PPIT ensemble\]\(#\) at the beginning of the instrumental period relative to preindustrial times \(\$\sim 1900\$ CE, Figure 3a\). Thus, the 67% and 81% of the land warming occurs after 1900 CE in the \[GST_Standard ensemble\]\(#\) and the \[GST_PPIT ensemble\]\(#\), respectively, indicating an accelerated land warming during the 20th century in agreement with other reconstructions of past changes in surface temperature \(Masson-Delmotte et al., 2013\).](#)

As in the case of surface temperature histories, the three approaches providing ground heat flux histories from BTP measurements are in good agreement during the entire period, although presenting higher uncertainties than for temperatures (Figure 3b and Table 1). Global results from Beltrami et al. (2002) are also displayed in Figure 3b (purple line), achieving similar values in comparison with [\[..⁶⁶ \]ground heat flux histories in the \[GHF_Standard\]\(#\), \[GHF_PPIT\]\(#\) and \[GHF_PPIF ensembles\]\(#\) except for the second half of the 20th century. Global heat flux change achieves \$70 \pm 20\$ mW m⁻², \$60 \pm 50\$ mW m⁻² and \$60 \pm 40\$ mW m⁻² for the \[\\[..⁶⁷ \\]GHF_Standard\]\(#\), \[GHF_PPIT\]\(#\) and \[GHF_PPIF ensembles\]\(#\), respectively \(Table 1\), in contrast to the \$39 \pm 4\$ mW m⁻² presented in Beltrami et al. \(2002\) and the \$\sim 33\$ mW m⁻² from Beltrami \(2002a\). The large number of recently acquired profiles included in our analysis may explain the larger flux estimates in comparison with previous works, since BTP measurements recorded before the 1980s did not capture the large disturbances in the surface energy budget from recent decades \(Stevens et al., 2008\). Global changes in \[\\[..⁶⁸ \\]ground heat content were estimated from the \\[GHF_Standard\\]\\(#\\), \\[GHF_PPIT\\]\\(#\\) and \\[GHF_PPIF ensembles\\]\\(#\\) by scaling these fluxes to the continental areas except Antarctica and Greenland, where there are no BTP measurements\\[..⁶⁹ \\], which results in three new sets of results: the \\[GHC_Standard\\]\\(#\\), \\[GHC_PPIT\\]\\(#\\) and \\[GHC_PPIF ensembles\\]\\(#\\). Changes in ground heat content of \\$15 \pm 5\\$ ZJ, \\$10 \pm 10\\$ ZJ and \\$13 \pm 8\\$ ZJ \\(1 ZJ = \\$10^{21}\\$ J\\) are obtained for the period 1950-2000 CE using the \\[\\\[..⁷⁰ \\\]GHC_Standard\\]\\(#\\), \\[GHC_PPIT\\]\\(#\\) and \\[GHC_PPIF ensembles\\]\\(#\\), \\[\\\[..⁷¹ \\\]\\]\\(#\\) respectively, in comparison with the \\$9 \pm 1\\$ ZJ in Beltrami et al. \\(2002\\) and the 7 ZJ in Beltrami \\(2002a\\). As expected, these estimates of continental heat storage are larger than previously reported since the heat flux histories also present higher values. The small uncertainty for heat flux histories, and therefore for estimates of continental heat storage, showed by the Standard and \\[\\\[..⁷²\\]\\(#\\)\]\(#\)](#)

⁶⁴removed: Standard approach

⁶⁵removed: GSTHs

⁶⁶removed: GHFHs derived by the Standard, PPIT and PPIF approaches

⁶⁷removed: Standard, PPIT and

⁶⁸removed: GHC were estimated for the Standard, PPIT and PPIF heat flux histories

⁶⁹removed: . GHCchanges

⁷⁰removed: Standard

⁷¹removed: PPIT and PPIF approaches,

⁷²removed: PPIT ensembles

350]PPI approaches at the beginning of the period (Figure 3) is artificially imposed by Equation 18, since the heat flux estimate for the first temporal step is set to zero by default. Therefore, the [..⁷³]GHF_PPIF and GHC_PPIF ensembles are providing a more realistic estimate of the uncertainty in the global [..⁷⁴]ground heat flux histories and ground heat content estimates for the first half of the period, with larger uncertainties for [..⁷⁵]all ensembles in the second half of the period.

355 Although the borehole database used here contains BTP measurements recorded after 2000 CE, results are shown until the end of the 20th century, since the number of available logs decreases sharply afterwards and the remaining profiles are located mainly at high latitudes in North America and Australia (Figure 1). We use the trend for the period 1970-2000 CE to extrapolate the heat flux histories until 2018 CE, providing with an estimate of the accumulated heat content in the continental subsurface from 1960 CE to the present (Figure 4). The global mean change of heat flux for the entire period is approximately 90 mW m⁻² considering all inversion approaches, while the global heat flux change since 2000 CE is ~ 120 mW m⁻². Thus, the accumulated heat within the global continental subsurface obtained from these flux estimates achieve 20 ZJ for the entire 360 period and ~ 9 ZJ for 2000-2018 CE. That is, if the global heat flux increase during the first decades of the 21st century resembled the trend of the period 1970-2000 CE, half of the total increase in energy storage within the continental subsurface in the last fifty-eight years would have occurred during the last two decades, a remarkably similar result in comparison with the accelerated ocean heat uptake in the last decades (Gleckler et al., 2016; Cheng et al., 2017, 2019).

5 Discussion

365 Ground surface temperature and ground heat flux histories retrieved by the three inversion models used here achieve similar evolutions since preindustrial times, and yield similar estimates of ground heat content for all continental areas without considering Antarctica and Greenland (Figures 3, S2 and S3, and Tables 1, S1 and S2). Nonetheless, the surface temperature, heat flux and heat storage results are larger than previous global estimates of [..⁷⁶]ground surface temperature histories, ground heat flux histories and ground heat content from borehole data (Pollack et al., 1998; Huang et al., 2000; Beltrami, 2002a; 370 Beltrami et al., 2002; Pollack and Smerdon, 2004). The main reason for the higher values reported here is the inclusion of additional temperature profiles measured at more recent dates than those employed in the literature, since logs acquired after the 1980s and 1990s recorded larger changes in the subsurface thermal regime due to larger variations in the surface energy balance (Stevens et al., 2008). That is, more than 250 high-quality logs have been measured or made available for the community since the early 2000s, including profiles from scarcely represented areas in the southern hemisphere. Additionally, there have 375 been improvements in the aggregation and treatment of borehole profiles contributing to the differences between our estimates and previous works (Beltrami et al., 2015b). We have truncated all logs to the same depth before performing the analysis in

⁷³removed: PPIF ensemble is

⁷⁴removed: GHFHs and GHC

⁷⁵removed: the three approaches

⁷⁶removed: GSTHs, GHFHs and GHC

contrast to previous studies, which used profiles including a range of bottom depths, therefore including [..⁷⁷] estimates of ground surface temperature histories and ground heat flux histories with different periods of reference.

The larger differences in uncertainties in heat flux estimates from the GHF_PPIT ensemble in comparison with those from the GHF_PPIF ensemble are caused by the criterium to discard unrealistic inversions in the PPI approach (Figures 3b, S2b and S3b). That is, the heat flux estimates for the GHF_PPIT ensemble were not filtered out using the flux criterium (0.51 W m^{-2}) of the PPI approach but the temperature criterium (2.57 K). Applying these different criteria is necessary since heat flux estimates from the GHF_PPIT ensemble result from applying Equation 18 to the previously retrieved surface temperature histories in the GST_PPIT ensemble, while the heat flux histories considered in the GHF_PPIF ensemble result from direct inversions of heat flux profiles, as explained in Section [..⁷⁸]3.3.3.

Borehole temperature profiles present a unique ability to integrate multi-centennial changes in the surface energy balance (Beltrami, 2002b), which makes borehole inversions an important source of information about preindustrial conditions. The depth range considered here (from 15 m to 300 m) allows to retrieve information from ~ 700 years before the logging date of each log, i.e., several centuries before the industrialization. Thus, all surface temperature histories displayed in Figures 3a, S2a and S3a are relative to approximately 1300-1700 CE, as the subsurface quasi-equilibrium profile is estimated here from the 200-300 m depth range for all profiles (Cuesta-Valero et al., 2019). The ground surface temperature increases relative to preindustrial conditions from the three GST_PPIT ensembles analyzed here are ~ 1.0 K for the last part of the 20th century [..⁷⁹], as previously shown in the Results section and Tables 1, S1 and S2 [..⁸⁰]. This is not, however, an estimate of the global temperature change, since land temperature changes at a higher pace than the temperature at the surface of the ocean due to their different thermal properties. The ratio between land temperature change and ocean temperature change is estimated in Harrison et al. (2015) based on an ensemble of long-term [..⁸¹] general circulation model simulations performed under different external forcings, resulting in land temperature changes ~ 2.36 times larger than ocean temperature changes. Thus, the corresponding ocean temperature change to the land temperature change retrieved from borehole temperature profiles can be approximated as ~ 0.4 K, which [..⁸²] suggests a global temperature change of ~ 0.7 K since preindustrial times. Such a temperature change from preindustrial conditions is in good agreement with the estimates of $0.55 - 0.8$ K discussed in Hawkins et al. (2017) using observations, [..⁸³] general circulation model simulations and proxy databases, even for a preindustrial period much further in the past in comparison with the periods analyzed in Schurer et al. (2017).

These new estimates of continental heat storage and ground heat flux from BTP inversions have implications for the assessment of the Earth's [..⁸⁴] heat inventory and for the comparison with [..⁸⁵] general circulation model simulations. The ocean heat flux is still much larger than the ground heat flux, with an ocean flux of $\sim 900 \pm 100 \text{ mW m}^{-2}$ (von Schuckmann

⁷⁷ removed: GSTH and GHFH estimates

⁷⁸ removed: ??

⁷⁹ removed: (

⁸⁰ removed:)

⁸¹ removed: CGCM

⁸² removed: yields an approximated global surface

⁸³ removed: CGCM

⁸⁴ removed: energy budget

⁸⁵ removed: CGCM simulations. Although the ocean

et al., 2020) in contrast to the $\sim 129 \pm 28 \text{ mW m}^{-2}$ of ground heat flux (Figure 4) for the period 1993-2018 CE. Nevertheless, although the ocean is still the largest component of the Earth's ^[.86]heat inventory (89%), the contribution of the continental subsurface is higher than previously reported (6% instead of 2-5%, von Schuckmann et al., 2020), reinforcing the necessity of monitoring and accounting for the rest of components of the inventory. Furthermore, previous assessments
410 have shown that ^[.87]general circulation model simulations are unable to represent changes in continental heat storage due to their shallow land surface model components (Stevens et al., 2007; MacDougall et al., 2008; Cuesta-Valero et al., 2016). The new ^[.88]estimates of continental heat storage emphasize the demand for deeper subsurfaces in ^[.89]general circulation model in order to generate global transient simulations capable of correctly reproducing the Earth's ^[.90]heat inventory.

The distribution of BTP measurements used in this analysis is specially scarce in zones of Africa, South America and the
415 Middle East, which may rise doubts about the global representativity of the assembled borehole dataset. Previous works have assessed the spatial distribution of BTP measurements using transient climate simulations performed by ^[.91]general circulation models at millennial time scales (González-Rouco et al., 2006; González-Rouco et al., 2009; García-García et al., 2016; Melo-Aguilar et al., 2019), and borehole databases aggregated using different techniques (Beltrami and Bourlon, 2004; Pollack and Smerdon, 2004), with all studies concluding that the effects of limited regional sampling on estimates of global changes
420 should be minor. Additionally, surface air temperatures from SAT_CRU data present markedly similar values considering both the full domain, and locations and dates containing BTP inversions (see red and orange lines in Figure 3), supporting the claim that borehole temporal and spatial distributions are representative of global conditions. Nevertheless, repeating measurements at borehole sites previously logged as well as obtaining new records at zones with reduced density of BTP data would improve the global estimates of ground surface temperature and ground heat flux histories from borehole temperature profiles.

425 6 Conclusions

The magnitude of the retrieved changes in ground surface temperature in this analysis supports the claim that the Earth's surface has warmed by $\sim 0.7 \text{ K}$ since preindustrial times. The new estimates also reveal that the continental subsurface has stored more energy during the last part of the 20th century than previously reported, reaching around 12 ZJ. This evidences the need for including deeper land surface model components in ^[.92]transient simulations performed by general circulation
430 models in order to correctly reproduce the land component of the Earth's ^[.93]heat inventory, as well as potentially powerful carbon feedbacks related to energy-dependent processes of the continental subsurface, such as the stability of the soil carbon pool and permafrost evolution.

⁸⁶removed: energy budget

⁸⁷removed: CGCM

⁸⁸removed: GHC estimates

⁸⁹removed: CGCMs

⁹⁰removed: energy budget

⁹¹removed: CGCMs

⁹²removed: CGCM transient simulations

⁹³removed: energy budget

Appendix A: Acronyms

Table A1. List of acronyms used in the main text.

Acronym	Definition
BTP	Borehole Temperature Profile
CE	Common Era
PPI	Perturbed Parameter Inversion
GST_PPIT	Ground Surface Temperature (GST) retrieved using the Perturbed Parameter Inversion (PPI) approach and subsurface temperature profiles (Section 3.3.2)
GST_Standard	Ground Surface Temperature (GST) retrieved using the Standard approach (Section 3.3.1)
GHF_PPIF	Ground Heat Flux (GHF) at the surface retrieved using the Perturbed Parameter Inversion (PPI) approach and subsurface flux profiles (Section 3.3.3)
GHF_PPIT	Ground Heat Flux (GHF) at the surface retrieved using the GST_PPIT ensemble and Equation 18
GHF_Standard	Ground Heat Flux (GHF) at the surface retrieved using the GST_Standard ensemble and Equation 18
GHC_PPIF	Ground Heat Content (GHC) retrieved using the GHF_PPIF ensemble
GHC_PPIT	Ground Heat Content (GHC) retrieved using the GHF_PPIT ensemble
GHC_Standard	Ground Heat Content (GHC) retrieved using the GHF_Standard ensemble
RMSE	Root Mean Square Error
SAT_CRU	Surface Air Temperature (SAT) from CRU TS 4.01 product
SVD	Singular Value Decomposition

Data availability. Data from the Climatic Research Unit (CRU) of East Anglia University can be accessed at <http://doi.org/10/gcmcz3>. Bore-
435 hole data can be downloaded from: NOAA server for a global dataset (<ftp://ftp.ncdc.noaa.gov/pub/data/paleo/borehole/>), Jaume-Santero et al. (2016) for North America (doi:10.6084/m9.figshare.2062140), Suman et al. (2017) for Tasmania (<https://doi.org/10.5194/cp-13-559-2017-supplement>), and Pickler et al. (2018) for Chile (doi:10.6084/m9.figshare.5220964.v2).

Author contributions. FJCV analyzed the borehole data, developed the PPI technique applied to characterize uncertainties in borehole inver-
440 sions, and produced all results and figures. All authors contributed to the interpretation and discussion of results. FJCV wrote the manuscript with continuous feedback from all authors.

Competing interests. The authors declare that they have no conflict of interest.

Acknowledgements. We are grateful for two anonymous reviewers and their thoughtful and constructive feedback. This work was supported by grants from the Natural Sciences and Engineering Research Council of Canada Discovery Grant (NSERC DG 140576948), the Canada Research Chairs Program (CRC 230687), and the Canada Foundation for Innovation (CFI) to H. Beltrami. H. Beltrami holds Canada
445 Research Chair in Climate Dynamics. A.G.G. and F.J.C.V. are funded by H. Beltrami's Canada Research Chair program, the School of Graduate Students at Memorial University of Newfoundland and the Research Office at St. Francis Xavier University.

References

- Barkaoui, A. E., Correia, A., Zarhloule, Y., Rimi, A., Carneiro, J., Boughriba, M., and Verdoya, M.: Reconstruction of remote climate change from borehole temperature measurement in the eastern part of Morocco, *Climatic Change*, 118, 431–441, <https://doi.org/10.1007/s10584-012-0638-7>, <https://doi.org/10.1007/s10584-012-0638-7>, 2013.
- 450 Beck, A.: Climatically perturbed temperature gradients and their effect on regional and continental heat-flow means, *Tectonophysics*, 41, 17–39, [https://doi.org/https://doi.org/10.1016/0040-1951\(77\)90178-0](https://doi.org/https://doi.org/10.1016/0040-1951(77)90178-0), <http://www.sciencedirect.com/science/article/pii/0040195177901780>, 1977.
- Beltrami, H.: Surface heat flux histories from inversion of geothermal data: Energy balance at the Earth's surface, *Journal of Geophysical Research: Solid Earth*, 106, 21 979–21 993, <https://doi.org/10.1029/2000JB000065>, <https://agupubs.onlinelibrary.wiley.com/doi/abs/10.1029/2000JB000065>, 2001.
- 455 Beltrami, H.: Climate from borehole data: Energy fluxes and temperatures since 1500, *Geophysical Research Letters*, 29, 26–1–26–4, <https://doi.org/10.1029/2002GL015702>, <http://dx.doi.org/10.1029/2002GL015702>, 2111, 2002a.
- Beltrami, H.: Earth's Long-Term Memory, *Science*, 297, 206–207, <https://doi.org/10.1126/science.1074027>, <https://science.sciencemag.org/content/297/5579/206>, 2002b.
- 460 Beltrami, H. and Bournon, E.: Ground warming patterns in the Northern Hemisphere during the last five centuries, *Earth and Planetary Science Letters*, 227, 169 – 177, <https://doi.org/http://dx.doi.org/10.1016/j.epsl.2004.09.014>, <http://www.sciencedirect.com/science/article/pii/S0012821X04005576>, 2004.
- Beltrami, H., Jessop, A. M., and Mareschal, J.-C.: Ground temperature histories in eastern and central Canada from geothermal measurements: evidence of climatic change, *Global and Planetary Change*, 6, 167 – 183, [https://doi.org/http://dx.doi.org/10.1016/0921-8181\(92\)90033-7](https://doi.org/http://dx.doi.org/10.1016/0921-8181(92)90033-7), <http://www.sciencedirect.com/science/article/pii/0921818192900337>, *climatic Change Inferred from Underground Temperatures*, 1992.
- 465 Beltrami, H., Smerdon, J. E., Pollack, H. N., and Huang, S.: Continental heat gain in the global climate system, *Geophysical Research Letters*, 29, 8–1–8–3, <https://doi.org/10.1029/2001GL014310>, <http://dx.doi.org/10.1029/2001GL014310>, 2002.
- 470 Beltrami, H., Bournon, E., Kellman, L., and González-Rouco, J. F.: Spatial patterns of ground heat gain in the Northern Hemisphere, *Geophysical Research Letters*, 33, n/a–n/a, <https://doi.org/10.1029/2006GL025676>, <http://dx.doi.org/10.1029/2006GL025676>, 106717, 2006.
- Beltrami, H., Matharoo, G. S., and Smerdon, J. E.: Ground surface temperature and continental heat gain: uncertainties from underground, *Environmental Research Letters*, 10, 014 009, <https://doi.org/10.1088/1748-9326/10/1/014009>, <https://doi.org/10.1088%2F1748-9326%2F10%2F1%2F014009>, 2015a.
- 475 Beltrami, H., Matharoo, G. S., and Smerdon, J. E.: Impact of borehole depths on reconstructed estimates of ground surface temperature histories and energy storage, *Journal of Geophysical Research: Earth Surface*, 120, 763–778, <https://doi.org/10.1002/2014JF003382>, <http://dx.doi.org/10.1002/2014JF003382>, 2014JF003382, 2015b.
- Beltrami, H., Matharoo, G. S., Smerdon, J. E., Illanes, L., and Tarasov, L.: Impacts of the Last Glacial Cycle on ground surface temperature reconstructions over the last millennium, *Geophysical Research Letters*, 44, 355–364, <https://doi.org/10.1002/2016GL071317>, <https://agupubs.onlinelibrary.wiley.com/doi/abs/10.1002/2016GL071317>, 2017.
- 480 Bodri, L. and Cermak, V.: Borehole temperatures, climate change and the pre-observational surface air temperature mean: allowance for hydraulic conditions, *Global and Planetary Change*, 45, 265 – 276, <https://doi.org/https://doi.org/10.1016/j.gloplacha.2004.09.001>, <http://www.sciencedirect.com/science/article/pii/S0921818104001225>, 2005.

- Bullard, E. C. and Schonland, B. F. J.: Heat flow in South Africa, *Proceedings of the Royal Society of London. Series A. Mathematical and Physical Sciences*, 173, 474–502, <https://doi.org/10.1098/rspa.1939.0159>, <https://royalsocietypublishing.org/doi/abs/10.1098/rspa.1939.0159>, 1939.
- Campbell, B. M., Vermeulen, S. J., Aggarwal, P. K., Corner-Dolloff, C., Girvetz, E., Loboguerrero, A. M., Ramirez-Villegas, J., Rosenstock, T., Sebastian, L., Thornton, P. K., and Wollenberg, E.: Reducing risks to food security from climate change, *Global Food Security*, 11, 34 – 43, <https://doi.org/https://doi.org/10.1016/j.gfs.2016.06.002>, <http://www.sciencedirect.com/science/article/pii/S2211912415300262>, 2nd International Global Food Security Conference, 2016.
- Carslaw, H. and Jaeger, J.: *Conduction of Heat in Solids*, Clarendon Press, Oxford, 1959.
- Cermak, V.: Underground temperature and inferred climatic temperature of the past millenium, *Palaeogeography, Palaeoclimatology, Palaeoecology*, 10, 1–19, [https://doi.org/https://doi.org/10.1016/0031-0182\(71\)90043-5](https://doi.org/https://doi.org/10.1016/0031-0182(71)90043-5), 1971.
- Cheng, L., Trenberth, K. E., Fasullo, J., Boyer, T., Abraham, J., and Zhu, J.: Improved estimates of ocean heat content from 1960 to 2015, *Science Advances*, 3, <https://doi.org/10.1126/sciadv.1601545>, <https://advances.sciencemag.org/content/3/3/e1601545>, 2017.
- Cheng, L., Abraham, J., Hausfather, Z., and Trenberth, K. E.: How fast are the oceans warming?, *Science*, 363, 128–129, <https://doi.org/10.1126/science.aav7619>, <https://science.sciencemag.org/content/363/6423/128>, 2019.
- Chouinard, C. and Mareschal, J.-C.: Ground surface temperature history in southern Canada: Temperatures at the base of the Laurentide ice sheet and during the Holocene, *Earth and Planetary Science Letters*, 277, 280 – 289, <https://doi.org/https://doi.org/10.1016/j.epsl.2008.10.026>, <http://www.sciencedirect.com/science/article/pii/S0012821X08006882>, 2009.
- Church, J. A., White, N. J., Konikow, L. F., Domingues, C. M., Cogley, J. G., Rignot, E., Gregory, J. M., van den Broeke, M. R., Monaghan, A. J., and Velicogna, I.: Revisiting the Earth’s sea-level and energy budgets from 1961 to 2008, *Geophysical Research Letters*, 38, n/a–n/a, <https://doi.org/10.1029/2011GL048794>, <http://dx.doi.org/10.1029/2011GL048794>, 118601, 2011.
- Clauser, C. and Mareschal, J.-C.: Ground temperature history in central Europe from borehole temperature data, *Geophysical Journal International*, 121, 805–817, <https://doi.org/10.1111/j.1365-246X.1995.tb06440.x>, <https://doi.org/10.1111/j.1365-246X.1995.tb06440.x>, 1995.
- Collins, M., Booth, B. B. B., Bhaskaran, B., Harris, G. R., Murphy, J. M., Sexton, D. M. H., and Webb, M. J.: Climate model errors, feedbacks and forcings: a comparison of perturbed physics and multi-model ensembles, *Climate Dynamics*, 36, 1737–1766, <https://doi.org/10.1007/s00382-010-0808-0>, <https://doi.org/10.1007/s00382-010-0808-0>, 2011.
- Cuesta-Valero, F. J., García-García, A., Beltrami, H., and Smerdon, J. E.: First assessment of continental energy storage in CMIP5 simulations, *Geophysical Research Letters*, pp. n/a–n/a, <https://doi.org/10.1002/2016GL068496>, <http://dx.doi.org/10.1002/2016GL068496>, 2016GL068496, 2016.
- Cuesta-Valero, F. J., García-García, A., Beltrami, H., Zorita, E., and Jaume-Santero, F.: Long-term Surface Temperature (LoST) database as a complement for GCM preindustrial simulations, *Climate of the Past*, 15, 1099–1111, <https://doi.org/10.5194/cp-15-1099-2019>, <https://www.clim-past.net/15/1099/2019/>, 2019.
- Davis, M. G., Harris, R. N., and Chapman, D. S.: Repeat temperature measurements in boreholes from northwestern Utah link ground and air temperature changes at the decadal time scale, *Journal of Geophysical Research: Solid Earth*, 115, <https://doi.org/10.1029/2009JB006875>, <https://agupubs.onlinelibrary.wiley.com/doi/abs/10.1029/2009JB006875>, 2010.
- Demezko, D. Y. and Gornostaeva, A. A.: Late Pleistocene–Holocene ground surface heat flux changes reconstructed from borehole temperature data (the Urals, Russia), *Climate of the Past*, 11, 647–652, <https://doi.org/10.5194/cp-11-647-2015>, <https://www.clim-past.net/11/647/2015/>, 2015.

- Dutton, A., Carlson, A. E., Long, A. J., Milne, G. A., Clark, P. U., DeConto, R., Horton, B. P., Rahmstorf, S., and Raymo, M. E.: Sea-level rise due to polar ice-sheet mass loss during past warm periods, *Science*, 349, <https://doi.org/10.1126/science.aaa4019>, <http://science.sciencemag.org/content/349/6244/aaa4019>, 2015.
- 525 Fernández-Donado, L., González-Rouco, J. F., Raible, C. C., Ammann, C. M., Barriopedro, D., García-Bustamante, E., Jungclaus, J. H., Lorenz, S. J., Luterbacher, J., Phipps, S. J., Servonnat, J., Swingedouw, D., Tett, S. F. B., Wagner, S., Yiou, P., and Zorita, E.: Large-scale temperature response to external forcing in simulations and reconstructions of the last millennium, *Climate of the Past*, 9, 393–421, <https://doi.org/10.5194/cp-9-393-2013>, <http://www.clim-past.net/9/393/2013/>, 2013.
- García-García, A., Cuesta-Valero, F. J., Beltrami, H., and Smerdon, J. E.: Simulation of air and ground temperatures in PMIP3/CMIP5 last millennium simulations: implications for climate reconstructions from borehole temperature profiles, *Environmental Research Letters*, 11, 044 022, <http://stacks.iop.org/1748-9326/11/i=4/a=044022>, 2016.
- 530 Gleckler, P. J., Durack, P. J., Stouffer, R. J., Johnson, G. C., and Forest, C. E.: Industrial-era global ocean heat uptake doubles in recent decades, *Nature Clim. Change*, 6, 394–398, <http://dx.doi.org/10.1038/nclimate2915>, 2016.
- González-Rouco, J. F., Beltrami, H., Zorita, E., and von Storch, H.: Simulation and inversion of borehole temperature profiles in surrogate climates: Spatial distribution and surface coupling, *Geophysical Research Letters*, 33, n/a–n/a, <https://doi.org/10.1029/2005GL024693>, <http://dx.doi.org/10.1029/2005GL024693>, 101703, 2006.
- 535 González-Rouco, J. F., Beltrami, H., Zorita, E., and Stevens, M. B.: Borehole climatology: a discussion based on contributions from climate modeling, *Climate of the Past*, 5, 97–127, <https://doi.org/10.5194/cp-5-97-2009>, <http://www.clim-past.net/5/97/2009/>, 2009.
- Hansen, J., Sato, M., Kharecha, P., and Schuckmann, K. v.: Earth’s energy imbalance and implications, *Atmospheric Chemistry and Physics*, 11, 13 421–13 449, 2011.
- 540 Harris, I., Jones, P., Osborn, T., and Lister, D.: Updated high-resolution grids of monthly climatic observations – the CRU TS3.10 Dataset, *International Journal of Climatology*, 34, 623–642, <https://doi.org/10.1002/joc.3711>, <http://dx.doi.org/10.1002/joc.3711>, 2014.
- Harris, R. N. and Chapman, D. S.: Mid-latitude (30°–60° N) climatic warming inferred by combining borehole temperatures with surface air temperatures, *Geophysical Research Letters*, 28, 747–750, <https://doi.org/10.1029/2000GL012348>, <http://dx.doi.org/10.1029/2000GL012348>, 2001.
- 545 Harrison, S. P., Bartlein, P. J., Izumi, K., Li, G., Annan, J., Hargreaves, J., Braconnot, P., and Kageyama, M.: Evaluation of CMIP5 palaeo-simulations to improve climate projections, *Nature Clim. Change*, 5, 735–743, <http://dx.doi.org/10.1038/nclimate2649>, 2015.
- Hartmann, A. and Rath, V.: Uncertainties and shortcomings of ground surface temperature histories derived from inversion of temperature logs, *Journal of Geophysics and Engineering*, 2, 299–311, <https://doi.org/10.1088/1742-2132/2/4/S02>, <https://doi.org/10.1088/1742-2132/2/4/S02>, 2005.
- 550 Hawkins, E., Ortega, P., Suckling, E., Schurer, A., Hegerl, G., Jones, P., Joshi, M., Osborn, T. J., Masson-Delmotte, V., Mignot, J., Thorne, P., and van Oldenborgh, G. J.: Estimating Changes in Global Temperature since the Preindustrial Period, *Bulletin of the American Meteorological Society*, 98, 1841–1856, <https://doi.org/10.1175/BAMS-D-16-0007.1>, <https://doi.org/10.1175/BAMS-D-16-0007.1>, 2017.
- Hicks Pries, C. E., Castanha, C., Porras, R. C., and Torn, M. S.: The whole-soil carbon flux in response to warming, *Science*, 355, 1420–1423, <https://doi.org/10.1126/science.aal1319>, <http://science.sciencemag.org/content/355/6332/1420>, 2017.
- 555 Hopcroft, P. O., Gallagher, K., and Pain, C. C.: Inference of past climate from borehole temperature data using Bayesian Reversible Jump Markov chain Monte Carlo, *Geophysical Journal International*, 171, 1430–1439, <https://doi.org/10.1111/j.1365-246X.2007.03596.x>, <https://doi.org/10.1111/j.1365-246X.2007.03596.x>, 2007.

- Huang, S., Pollack, H. N., and Shen, P.-Y.: Temperature trends over the past five centuries reconstructed from borehole temperatures, *Nature*, 403, 756–758, <http://dx.doi.org/10.1038/35001556>, 2000.
- 560 Irving, D. B., Wijffels, S., and Church, J. A.: Anthropogenic Aerosols, Greenhouse Gases, and the Uptake, Transport, and Storage of Excess Heat in the Climate System, *Geophysical Research Letters*, 46, 4894–4903, <https://doi.org/10.1029/2019GL082015>, <https://agupubs.onlinelibrary.wiley.com/doi/abs/10.1029/2019GL082015>, 2019.
- Jacob, T., Wahr, J., Pfeffer, W. T., and Swenson, S.: Recent contributions of glaciers and ice caps to sea level rise, *Nature*, 482, 514–518, <http://dx.doi.org/10.1038/nature10847>, 2012.
- 565 Jaume-Santero, F., Pickler, C., Beltrami, H., and Mareschal, J.-C.: North American regional climate reconstruction from ground surface temperature histories, *Climate of the Past*, 12, 2181–2194, <https://doi.org/10.5194/cp-12-2181-2016>, <http://www.clim-past.net/12/2181/2016/>, 2016.
- Johnson, G. C., Lyman, J. M., and Loeb, N. G.: Improving estimates of Earth’s energy imbalance, *Nature Climate Change*, 6, 639 EP –, <https://doi.org/10.1038/nclimate3043>, 2016.
- 570 Knutti, R., Sedláček, J., Sanderson, B. M., Lorenz, R., Fischer, E. M., and Eyring, V.: A climate model projection weighting scheme accounting for performance and interdependence, *Geophysical Research Letters*, 44, 1909–1918, <https://doi.org/10.1002/2016GL072012>, <https://agupubs.onlinelibrary.wiley.com/doi/abs/10.1002/2016GL072012>, 2017.
- Kundzewicz, Z. W., Kanae, S., Seneviratne, S. I., Handmer, J., Nicholls, N., Peduzzi, P., Mechler, R., Bouwer, L. M., Arnell, N., Mach, K., Muir-Wood, R., Brakenridge, G. R., Kron, W., Benito, G., Honda, Y., Takahashi, K., and Sherstyukov, B.: Flood risk and climate change: global and regional perspectives, *Hydrological Sciences Journal*, 59, 1–28, <https://doi.org/10.1080/02626667.2013.857411>, <https://doi.org/10.1080/02626667.2013.857411>, 2014.
- Lachenbruch, A. H. and Marshall, B. V.: Changing Climate: Geothermal Evidence from Permafrost in the Alaskan Arctic, *Science*, 234, 689–696, <https://doi.org/10.1126/science.234.4777.689>, <http://science.sciencemag.org/content/234/4777/689>, 1986.
- Lanczos, C.: *Linear differential operators*, Van Nostrand, New York, 1961.
- 580 Lane, A. C.: Geotherms of Lake Superior Copper Country, *GSA Bulletin*, 34, 703–720, <https://doi.org/10.1130/GSAB-34-703>, <https://doi.org/10.1130/GSAB-34-703>, 1923.
- Lembo, V., Folini, D., Wild, M., and Lionello, P.: Inter-hemispheric differences in energy budgets and cross-equatorial transport anomalies during the 20th century, *Climate Dynamics*, 53, 115–135, <https://doi.org/10.1007/s00382-018-4572-x>, <https://doi.org/10.1007/s00382-018-4572-x>, 2019.
- 585 Lesperance, M., Smerdon, J. E., and Beltrami, H.: Propagation of linear surface air temperature trends into the terrestrial subsurface, *Journal of Geophysical Research: Atmospheres*, 115, n/a–n/a, <https://doi.org/10.1029/2010JD014377>, <http://dx.doi.org/10.1029/2010JD014377>, d21115, 2010.
- Levitus, S., Antonov, J., and Boyer, T.: Warming of the world ocean, 1955–2003, *Geophysical Research Letters*, 32, n/a–n/a, <https://doi.org/10.1029/2004GL021592>, <http://dx.doi.org/10.1029/2004GL021592>, 102604, 2005.
- 590 Levy, K., Woster, A. P., Goldstein, R. S., and Carlton, E. J.: Untangling the Impacts of Climate Change on Waterborne Diseases: a Systematic Review of Relationships between Diarrheal Diseases and Temperature, Rainfall, Flooding, and Drought, *Environmental Science & Technology*, 50, 4905–4922, <https://doi.org/10.1021/acs.est.5b06186>, <https://doi.org/10.1021/acs.est.5b06186>, PMID: 27058059, 2016.
- Lloyd, S. J., Kovats, R. S., and Chalabi, Z.: Climate Change, Crop Yields, and Undernutrition: Development of a Model to Quantify the Impact of Climate Scenarios on Child Undernutrition, *Environmental Health Perspectives*, 119, 1817–1823, <https://doi.org/10.1289/ehp.1003311>, <https://ehp.niehs.nih.gov/doi/abs/10.1289/ehp.1003311>, 2011.
- 595

- Loeb, N. G., Wang, H., Cheng, A., Kato, S., Fasullo, J. T., Xu, K.-M., and Allan, R. P.: Observational constraints on atmospheric and oceanic cross-equatorial heat transports: revisiting the precipitation asymmetry problem in climate models, *Climate Dynamics*, 46, 3239–3257, <https://doi.org/10.1007/s00382-015-2766-z>, <https://doi.org/10.1007/s00382-015-2766-z>, 2016.
- MacDougall, A. H., González-Rouco, J. F., Stevens, M. B., and Beltrami, H.: Quantification of subsurface heat storage in a GCM simulation, *Geophysical Research Letters*, 35, n/a–n/a, <https://doi.org/10.1029/2008GL034639>, <http://dx.doi.org/10.1029/2008GL034639>, 2008.
- MacDougall, A. H., Beltrami, H., González-Rouco, J. F., Stevens, M. B., and Bourlon, E.: Comparison of observed and general circulation model derived continental subsurface heat flux in the Northern Hemisphere, *Journal of Geophysical Research: Atmospheres* (1984–2012), 115, 2010.
- MacDougall, A. H., Avis, C. A., and Weaver, A. J.: Significant contribution to climate warming from the permafrost carbon feedback, *Nature Geosci*, 5, 719–721, <https://doi.org/10.1038/ngeo1573>, <http://dx.doi.org/10.1038/ngeo1573>, 2012.
- Mareschal, J.-C. and Beltrami, H.: Evidence for recent warming from perturbed geothermal gradients: examples from eastern Canada, *Climate Dynamics*, 6, 135–143, <https://doi.org/10.1007/BF00193525>, <http://dx.doi.org/10.1007/BF00193525>, 1992.
- Masson-Delmotte, V., Schulz, M., Abe-Ouchi, A., Beer, J., Ganopolski, A., González Rouco, J., Jansen, E., Lambeck, K., Luterbacher, J., Naish, T., Osborn, T., Otto-Bliesner, B., Quinn, T., Ramesh, R., Rojas, M., Shao, X., and Timmermann, A.: Information from Paleoclimate Archives, in: *Climate Change 2013: The Physical Science Basis. Contribution of Working Group I to the Fifth Assessment Report of the Intergovernmental Panel on Climate Change*, edited by Stocker, T., Qin, D., Plattner, G.-K., Tignor, M., Allen, S., Boschung, J., Nauels, A., Xia, Y., Bex, V., and Midgley, P., book section 5, pp. 383–464, Cambridge University Press, Cambridge, United Kingdom and New York, NY, USA, <https://doi.org/10.1017/CBO9781107415324.013>, www.climatechange2013.org, 2013.
- Matthews, T. K. R., Wilby, R. L., and Murphy, C.: Communicating the deadly consequences of global warming for human heat stress, *Proceedings of the National Academy of Sciences*, 114, 3861–3866, <https://doi.org/10.1073/pnas.1617526114>, <https://www.pnas.org/content/114/15/3861>, 2017.
- McGranahan, G., Balk, D., and Anderson, B.: The rising tide: assessing the risks of climate change and human settlements in low elevation coastal zones, *Environment and Urbanization*, 19, 17–37, <https://doi.org/10.1177/0956247807076960>, <https://doi.org/10.1177/0956247807076960>, 2007.
- McPherson, M., García-García, A., Cuesta-Valero, F. J., Beltrami, H., Hansen-Ketchum, P., MacDougall, D., and Ogden, N. H.: Expansion of the Lyme Disease Vector *Ixodes Scapularis* in Canada Inferred from CMIP5 Climate Projections, *Environmental Health Perspectives*, 125, 057 008, <https://doi.org/10.1289/EHP57>, <https://ehp.niehs.nih.gov/doi/abs/10.1289/EHP57>, 2017.
- Melo-Aguilar, C., González-Rouco, J. F., García-Bustamante, E., Steinert, N., Jungclaus, J. H., Navarro, J., and Roldan-Gómez, P. J.: Methodological and physical biases in global to sub-continental borehole temperature reconstructions: an assessment from a pseudo-proxy perspective, *Climate of the Past Discussions*, 2019, 1–31, <https://doi.org/10.5194/cp-2019-120>, <https://www.clim-past-discuss.net/cp-2019-120/>, 2019.
- Mottaghy, D. and Rath, V.: Latent heat effects in subsurface heat transport modelling and their impact on palaeotemperature reconstructions, *Geophysical Journal International*, 164, 236–245, <https://doi.org/10.1111/j.1365-246X.2005.02843.x>, <https://doi.org/10.1111/j.1365-246X.2005.02843.x>, 2006.
- NOAA: Borehole Database at National Oceanic and Atmospheric Administration’s Server, <https://www.ncdc.noaa.gov/data-access/paleoclimatology-data/datasets/borehole> [Last accessed September 2019], 2019.
- Oppenheimer, M., Glavovic, B., Hinkel, J., van de Wal, R., Magnan, A., Abd-Elgawad, A., Cai, R., Cifuentes-Jara, M., DeConto, R., Ghosh, T., Hay, J., Isla, F., Marzeion, B., Meyssignac, B., and Sebesvari, Z.: Sea Level Rise and Implications for Low-Lying Islands, Coasts

- and Communities, in: IPCC Special Report on the Ocean and Cryosphere in a Changing Climate, edited by Pörtner, H.-O., Roberts, D.,
635 Masson-Delmotte, V., Zhai, P., Tignor, M., Poloczanska, E., Mintenbeck, K., Alegría, A., Nicolai, M., Okem, A., Petzold, J., Rama, B.,
and Weyer, N., book section 4, pp. 321–446, In press, 2019.
- Palmer, M. D. and McNeall, D. J.: Internal variability of Earth’s energy budget simulated by CMIP5 climate models, *Environmental Research
Letters*, 9, 034016, <http://stacks.iop.org/1748-9326/9/i=3/a=034016>, 2014.
- Palmer, M. D., McNeall, D. J., and Dunstone, N. J.: Importance of the deep ocean for estimating decadal changes in Earth’s radiation
640 balance, *Geophysical Research Letters*, 38, n/a–n/a, <https://doi.org/10.1029/2011GL047835>, <http://dx.doi.org/10.1029/2011GL047835>,
113707, 2011.
- Phalkey, R. K., Aranda-Jan, C., Marx, S., Höfle, B., and Sauerborn, R.: Systematic review of current efforts to quantify
the impacts of climate change on undernutrition, *Proceedings of the National Academy of Sciences*, 112, E4522–E4529,
<https://doi.org/10.1073/pnas.1409769112>, <https://www.pnas.org/content/112/33/E4522>, 2015.
- 645 Pickler, C., Beltrami, H., and Mareschal, J.-C.: Laurentide Ice Sheet basal temperatures during the last glacial cycle as inferred from borehole
data, *Climate of the Past*, 12, 115–127, <https://doi.org/10.5194/cp-12-115-2016>, <http://www.clim-past.net/12/115/2016/>, 2016.
- Pickler, C., Gurza Fausto, E., Beltrami, H., Mareschal, J.-C., Suárez, F., Chacon-Oecklers, A., Blin, N., Cortés Calderón, M. T., Montenegro,
A., Harris, R., and Tassara, A.: Recent climate variations in Chile: constraints from borehole temperature profiles, *Climate of the Past*, 14,
559–575, <https://doi.org/10.5194/cp-14-559-2018>, <https://www.clim-past.net/14/559/2018/>, 2018.
- 650 Pollack, H. N. and Smerdon, J. E.: Borehole climate reconstructions: Spatial structure and hemispheric averages, *Journal of Geophysical
Research: Atmospheres*, 109, n/a–n/a, <https://doi.org/10.1029/2003JD004163>, <http://dx.doi.org/10.1029/2003JD004163>, d11106, 2004.
- Pollack, H. N., Huang, S., and Shen, P.-Y.: Climate Change Record in Subsurface Temperatures: A Global Perspective, *Science*, 282, 279–
281, <https://doi.org/10.1126/science.282.5387.279>, <https://science.sciencemag.org/content/282/5387/279>, 1998.
- Rath, V., González Rouco, J. F., and Goosse, H.: Impact of postglacial warming on borehole reconstructions of last millennium temperatures,
655 *Climate of the Past*, 8, 1059–1066, <https://doi.org/10.5194/cp-8-1059-2012>, <https://www.clim-past.net/8/1059/2012/>, 2012.
- Reiter, M.: Possible Ambiguities in Subsurface Temperature Logs: Consideration of Ground-water Flow and Ground Surface Tem-
perature Change, *pure and applied geophysics*, 162, 343–355, <https://doi.org/10.1007/s00024-004-2604-4>, <https://doi.org/10.1007/s00024-004-2604-4>, 2005.
- Riser, S. C., Freeland, H. J., Roemmich, D., Wijffels, S., Troisi, A., Belbéoch, M., Gilbert, D., Xu, J., Pouliquen, S., Thresher, A., Le Traon,
660 P.-Y., Maze, G., Klein, B., Ravichandran, M., Grant, F., Poulain, P.-M., Suga, T., Lim, B., Sterl, A., Sutton, P., Mork, K.-A., Vélez-Belchí,
P. J., Anson, I., King, B., Turton, J., Baringer, M., and Jayne, S. R.: Fifteen years of ocean observations with the global Argo array,
Nature Climate Change, 6, 145–153, <https://doi.org/10.1038/nclimate2872>, <https://doi.org/10.1038/nclimate2872>, 2016.
- Rosenzweig, C., Elliott, J., Deryng, D., Ruane, A. C., Müller, C., Arneth, A., Boote, K. J., Folberth, C., Glotter, M., Khabarov, N., Neumann,
K., Piontek, F., Pugh, T. A. M., Schmid, E., Stehfest, E., Yang, H., and Jones, J. W.: Assessing agricultural risks of climate change in
665 the 21st century in a global gridded crop model intercomparison, *Proceedings of the National Academy of Sciences*, 111, 3268–3273,
<https://doi.org/10.1073/pnas.1222463110>, <https://www.pnas.org/content/111/9/3268>, 2014.
- Roy, S., Harris, R. N., Rao, R. U. M., and Chapman, D. S.: Climate change in India inferred from geothermal observations, *Journal of Geo-
physical Research: Solid Earth*, 107, ETG 5–1–ETG 5–16, <https://doi.org/10.1029/2001JB000536>, <https://agupubs.onlinelibrary.wiley.com/doi/abs/10.1029/2001JB000536>, 2002.

- 670 Schurer, A. P., Mann, M. E., Hawkins, E., Tett, S. F. B., and Hegerl, G. C.: Importance of the pre-industrial baseline for likelihood of exceeding Paris goals, *Nature Climate Change*, 7, 563–567, <https://doi.org/10.1038/nclimate3345>, <https://doi.org/10.1038/nclimate3345>, 2017.
- Screen, J. A., Deser, C., Smith, D. M., Zhang, X., Blackport, R., Kushner, P. J., Oudar, T., McCusker, K. E., and Sun, L.: Consistency and discrepancy in the atmospheric response to Arctic sea-ice loss across climate models, *Nature Geoscience*, 11, 155–163, <https://doi.org/10.1038/s41561-018-0059-y>, <https://doi.org/10.1038/s41561-018-0059-y>, 2018.
- 675 Shen, P., Wang, K., Beltrami, H., and Mareschal, J.-C.: A comparative study of inverse methods for estimating climatic history from borehole temperature data, *Global and Planetary Change*, 6, 113 – 127, [https://doi.org/https://doi.org/10.1016/0921-8181\(92\)90030-E](https://doi.org/https://doi.org/10.1016/0921-8181(92)90030-E), <http://www.sciencedirect.com/science/article/pii/092181819290030E>, climatic Change Inferred from Underground Temperatures, 1992.
- Sherwood, S. C. and Huber, M.: An adaptability limit to climate change due to heat stress, *Proceedings of the National Academy of Sciences*, 680 107, 9552–9555, <https://doi.org/10.1073/pnas.0913352107>, <https://www.pnas.org/content/107/21/9552>, 2010.
- Stephens, G. L., Li, J., Wild, M., Clayson, C. A., Loeb, N., Kato, S., L’Ecuyer, T., Stackhouse, P. W., Lebsock, M., and Andrews, T.: An update on Earth’s energy balance in light of the latest global observations, *Nature Geoscience*, 5, 691–696, <https://doi.org/10.1038/ngeo1580>, <https://doi.org/10.1038/ngeo1580>, 2012.
- Stevens, M. B., Smerdon, J. E., González-Rouco, J. F., Stieglitz, M., and Beltrami, H.: Effects of bottom boundary placement on subsurface heat storage: Implications for climate model simulations, *Geophysical Research Letters*, 34, n/a–n/a, <https://doi.org/10.1029/2006GL028546>, <http://dx.doi.org/10.1029/2006GL028546>, 102702, 2007.
- 685 Stevens, M. B., González-Rouco, J. F., and Beltrami, H.: North American climate of the last millennium: Underground temperatures and model comparison, *Journal of Geophysical Research: Earth Surface*, 113, n/a–n/a, <https://doi.org/10.1029/2006JF000705>, <http://dx.doi.org/10.1029/2006JF000705>, f01008, 2008.
- 690 Suman, A., Dyer, F., and White, D.: Late Holocene temperature variability in Tasmania inferred from borehole temperature data, *Climate of the Past*, 13, 559–572, <https://doi.org/10.5194/cp-13-559-2017>, <https://www.clim-past.net/13/559/2017/>, 2017.
- Tomas, R. A., Deser, C., and Sun, L.: The Role of Ocean Heat Transport in the Global Climate Response to Projected Arctic Sea Ice Loss, *Journal of Climate*, 29, 6841–6859, <https://doi.org/10.1175/JCLI-D-15-0651.1>, <https://doi.org/10.1175/JCLI-D-15-0651.1>, 2016.
- Trenberth, K. E., Zhang, Y., Fasullo, J. T., and Cheng, L.: Observation-Based Estimates of Global and Basin Ocean Meridional Heat Transport 695 Time Series, *Journal of Climate*, 32, 4567–4583, <https://doi.org/10.1175/JCLI-D-18-0872.1>, <https://doi.org/10.1175/JCLI-D-18-0872.1>, 2019.
- Turcotte, D. L. and Schubert, G.: *Geodynamics*, Cambridge University Press, 2nd edition edn., 2002.
- Vasseur, G., Bernard, P., de Meulebrouck, J. V., Kast, Y., and Jolivet, J.: Holocene paleotemperatures deduced from geothermal measurements, *Palaeogeography, Palaeoclimatology, Palaeoecology*, 43, 237 – 259, [https://doi.org/https://doi.org/10.1016/0031-0182\(83\)90013-5](https://doi.org/https://doi.org/10.1016/0031-0182(83)90013-5), <http://www.sciencedirect.com/science/article/pii/0031018283900135>, 1983.
- 700 Vaughan, D., Comiso, J., Allison, I., Carrasco, J., Kaser, G., Kwok, R., Mote, P., Murray, T., Paul, F., Ren, J., Rignot, E., Solomina, O., Steffen, K., and Zhang, T.: Observations: Cryosphere, in: *Climate Change 2013: The Physical Science Basis. Contribution of Working Group I to the Fifth Assessment Report of the Intergovernmental Panel on Climate Change*, edited by Stocker, T., Qin, D., Plattner, G.-K., Tignor, M., Allen, S., Boschung, J., Nauels, A., Xia, Y., Bex, V., and Midgley, P., book section 4, pp. 317–382, Cambridge University Press, 705 Cambridge, United Kingdom and New York, NY, USA, <https://doi.org/10.1017/CBO9781107415324.012>, www.climatechange2013.org, 2013.

- von Schuckmann, K., Palmer, M. D., Trenberth, K. E., Cazenave, A., Chambers, D., Champollion, N., Hansen, J., Josey, S. A., Loeb, N., Mathieu, P. P., Meyssignac, B., and Wild, M.: An imperative to monitor Earth's energy imbalance, *Nature Climate Change*, 6, 138 EP –, <http://dx.doi.org/10.1038/nclimate2876>, 2016.
- 710 von Schuckmann, K., Cheng, L., Palmer, M. D., Hansen, J., Tassone, C., Aich, V., Adusumilli, S., Beltrami, H., Boyer, T., Cuesta-Valero, F. J., Desbruyères, D., Domingues, C., García-García, A., Gentine, P., Gilson, J., Gorfer, M., Haimberger, L., Ishii, M., Johnson, G. C., Killick, R., King, B. A., Kirchengast, G., Kolodziejczyk, N., Lyman, J., Marzeion, B., Mayer, M., Monier, M., Monselesan, D. P., Purkey, S., Roemmich, D., Schweiger, A., Seneviratne, S. I., Shepherd, A., Slater, D. A., Steiner, A. K., Straneo, F., Timmermans, M.-L., and Wijffels, S. E.: Heat stored in the Earth system: where does the energy go?, *Earth System Science Data*, 12, 2013–2041, <https://doi.org/10.5194/essd-12-2013-2020>, <https://essd.copernicus.org/articles/12/2013/2020/>, 2020.
- 715 Wang, J. and Bras, R.: Ground heat flux estimated from surface soil temperature, *Journal of Hydrology*, 216, 214 – 226, [https://doi.org/https://doi.org/10.1016/S0022-1694\(99\)00008-6](https://doi.org/https://doi.org/10.1016/S0022-1694(99)00008-6), <http://www.sciencedirect.com/science/article/pii/S0022169499000086>, 1999.
- Watts, N., Amann, M., Arnell, N., Ayeb-Karlsson, S., Belesova, K., Boykoff, M., Byass, P., Cai, W., Campbell-Lendrum, D., Capstick, S., Chambers, J., Dalin, C., Daly, M., Dasandi, N., Davies, M., Drummond, P., Dubrow, R., Ebi, K. L., Eckelman, M., Ekins, P., Escobar, L. E., Fernandez Montoya, L., Georgeson, L., Graham, H., Haggard, P., Hamilton, I., Hartinger, S., Hess, J., Kelman, I., Kiesewetter, G., Kjellstrom, T., Kniveton, D., Lemke, B., Liu, Y., Lott, M., Lowe, R., Sewe, M. O., Martinez-Urtaza, J., Maslin, M., McAllister, L., McGushin, A., Jankin Mikhaylov, S., Milner, J., Moradi-Lakeh, M., Morrissey, K., Murray, K., Munzert, S., Nilsson, M., Neville, T., Oreszczyn, T., Owfi, F., Pearman, O., Pencheon, D., Phung, D., Pye, S., Quinn, R., Rabbaniha, M., Robinson, E., Rocklöv, J., Semenza, J. C., Sherman, J., Shumake-Guillemot, J., Tabatabaei, M., Taylor, J., Trinanes, J., Wilkinson, P., Costello, A., Gong, P., and Montgomery, H.: The 2019 report of The Lancet Countdown on health and climate change: ensuring that the health of a child born today is not defined by a changing climate, *The Lancet*, 394, 1836–1878, [https://doi.org/10.1016/S0140-6736\(19\)32596-6](https://doi.org/10.1016/S0140-6736(19)32596-6), [https://doi.org/10.1016/S0140-6736\(19\)32596-6](https://doi.org/10.1016/S0140-6736(19)32596-6), 2019.
- 720 J. C., Sherman, J., Shumake-Guillemot, J., Tabatabaei, M., Taylor, J., Trinanes, J., Wilkinson, P., Costello, A., Gong, P., and Montgomery, H.: The 2019 report of The Lancet Countdown on health and climate change: ensuring that the health of a child born today is not defined by a changing climate, *The Lancet*, 394, 1836–1878, [https://doi.org/10.1016/S0140-6736\(19\)32596-6](https://doi.org/10.1016/S0140-6736(19)32596-6), [https://doi.org/10.1016/S0140-6736\(19\)32596-6](https://doi.org/10.1016/S0140-6736(19)32596-6), 2019.
- 725 Wu, X., Lu, Y., Zhou, S., Chen, L., and Xu, B.: Impact of climate change on human infectious diseases: Empirical evidence and human adaptation, *Environment International*, 86, 14 – 23, <https://doi.org/https://doi.org/10.1016/j.envint.2015.09.007>, <http://www.sciencedirect.com/science/article/pii/S0160412015300489>, 2016.
- 730

Table 1. Global mean estimates of ground surface temperature (GST), ground heat flux at the surface (GHF) and ground heat content within continental subsurface (GHC) from borehole temperature profiles. Values display the mean and 95% confidence interval for each time period from estimates using the [..⁹⁴]standard inversion approach (Standard), the new PPI approach [..⁹⁵]applied to [..⁹⁶]temperature and heat flux profiles (PPIT and PPIF, respectively). All the inversions were performed using a model of 25 years per time step. Temperatures in K, fluxes in mW m^{-2} and heat content in ZJ.

Period (CE)	Temperatures		Heat Fluxes			Heat Storage		
	GST_Standard	GST_PPIT	GHF_Standard	GHF_PPIT	GHF_PPIF	GHC_Standard	GHC_PPI	GHC_PPIF
1975-2000	1.2 ± 0.2	1.1 ± 0.3	100 ± 20	70 ± 70	80 ± 40	10 ± 2	8 ± 8	9 ± 5
1950-1975	0.8 ± 0.2	0.8 ± 0.5	40 ± 40	40 ± 80	40 ± 60	4 ± 4	4 ± 8	4 ± 6
1925-1950	0.6 ± 0.2	0.6 ± 0.6	30 ± 30	40 ± 60	30 ± 60	3 ± 4	4 ± 7	3 ± 6
1900-1925	0.5 ± 0.3	0.4 ± 0.5	30 ± 20	30 ± 40	20 ± 50	3 ± 2	3 ± 4	2 ± 5
1875-1900	0.4 ± 0.3	0.3 ± 0.5	30 ± 20	20 ± 40	20 ± 40	3 ± 2	2 ± 4	2 ± 5
1850-1875	0.3 ± 0.3	0.2 ± 0.5	20 ± 20	10 ± 30	10 ± 40	2 ± 2	1 ± 3	1 ± 4
1825-1850	0.2 ± 0.3	0.1 ± 0.4	20 ± 20	9 ± 30	10 ± 30	2 ± 2	0.9 ± 3	1 ± 3
1800-1825	0.1 ± 0.2	0.07 ± 0.3	10 ± 20	6 ± 20	7 ± 20	1 ± 2	0.7 ± 3	0.8 ± 2
1775-1800	0.04 ± 0.2	0.03 ± 0.3	10 ± 20	5 ± 20	5 ± 20	1 ± 2	0.5 ± 2	0.5 ± 2
1750-1775	-0.007 ± 0.1	0.002 ± 0.3	7 ± 10	3 ± 20	3 ± 20	0.7 ± 1	0.4 ± 2	0.3 ± 2
1725-1750	-0.04 ± 0.07	-0.02 ± 0.3	5 ± 10	3 ± 10	2 ± 20	0.5 ± 1	0.3 ± 1	0.2 ± 3
1700-1725	-0.07 ± 0.04	-0.03 ± 0.3	3 ± 9	2 ± 10	1 ± 30	0.3 ± 0.9	0.2 ± 1	0.1 ± 3
1675-1700	-0.08 ± 0.06	-0.04 ± 0.3	2 ± 7	1 ± 8	0.7 ± 30	0.2 ± 0.7	0.1 ± 0.8	0.07 ± 3
1650-1675	-0.10 ± 0.08	-0.04 ± 0.3	1 ± 5	0.9 ± 6	0.3 ± 30	0.1 ± 0.5	0.09 ± 0.6	0.03 ± 3
1625-1650	-0.1 ± 0.1	-0.05 ± 0.3	0.6 ± 4	0.5 ± 4	0.07 ± 30	0.07 ± 0.4	0.05 ± 0.4	0.007 ± 4
1600-1625	-0.1 ± 0.1	-0.05 ± 0.3	0.08 ± 2	0.2 ± 2	-0.2 ± 40	0.009 ± 0.2	0.02 ± 0.2	-0.02 ± 4

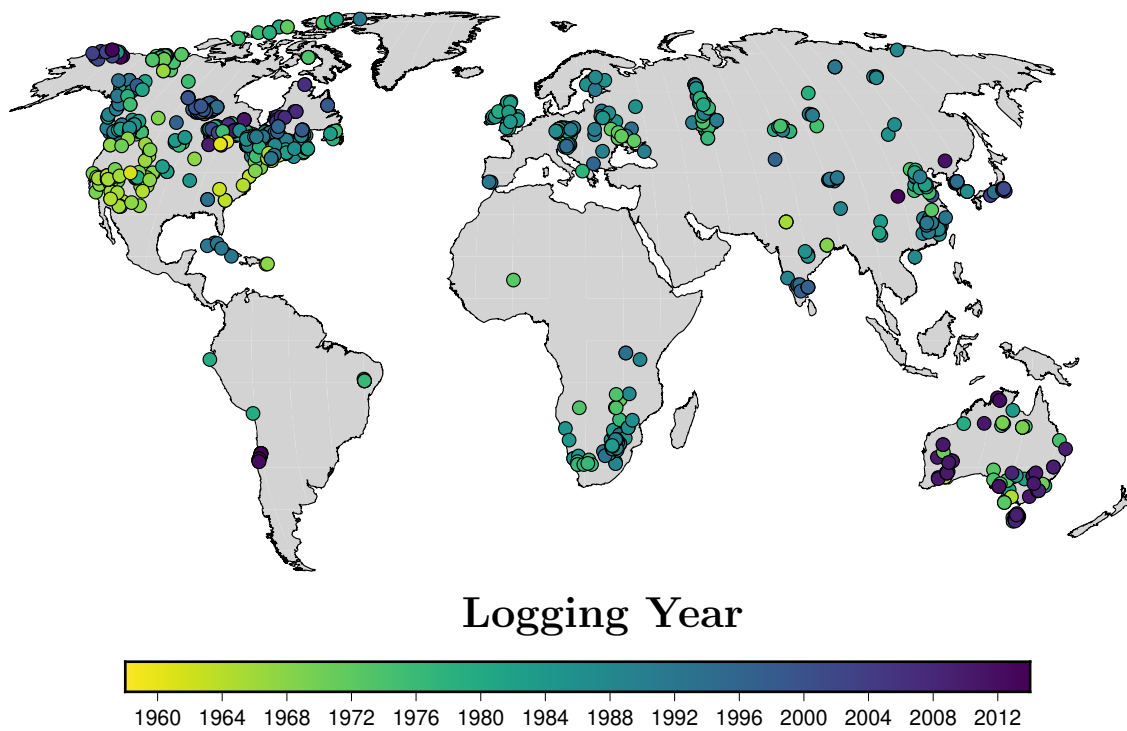


Figure 1. Logging years of the 1079 boreholes considered in the analysis.

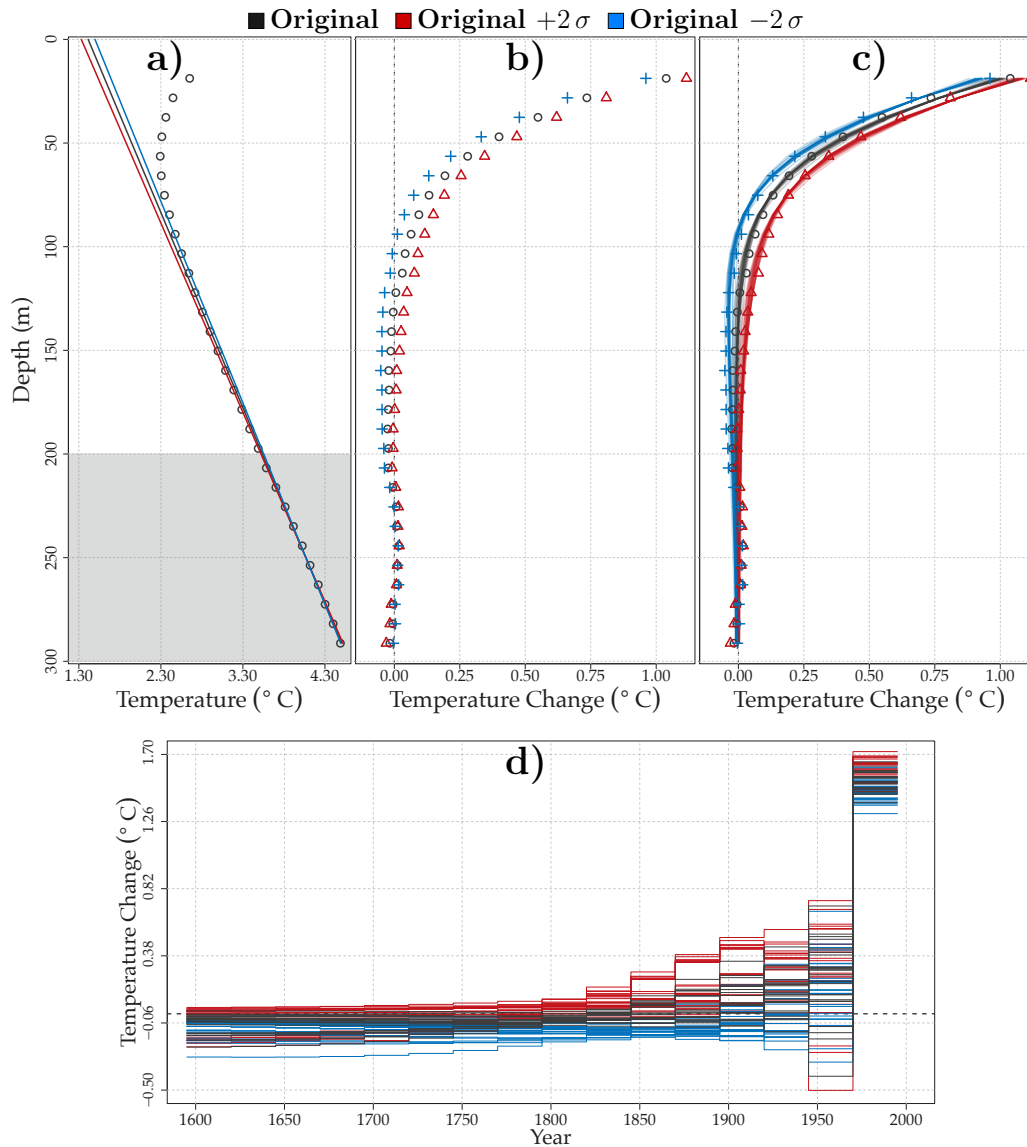


Figure 2. Borehole temperature profile measurements at Fox Mine (CA_9519), Manitoba (Canada) as an example to explain the inversion approaches in this study. (a) Observed original profile (black dots) as well as the estimated subsurface quasi-equilibrium temperature profile (black line) and the two extremal temperature profiles (red and blue lines) displaying the [..⁹⁷] error in determining the quasi-equilibrium profile. All three equilibrium profiles were estimated from the linear regression analysis of the deepest part of the measured profile (from 200 m to 300 m, grey zone). (b) Anomaly profiles estimated by subtracting the three equilibrium profiles to the original temperature profile. (c) As in (b), but including the 243 synthetic profiles generated from the corresponding ground surface temperature histories constituting the PPI ensemble of this borehole (red, blue and black shades). (d) Final ensemble of ground surface temperature histories considered for estimating the 5th, 50th and 95th weighted percentiles for this borehole. Each history is weighted depending on its performance against the corresponding anomaly profile (panel c).

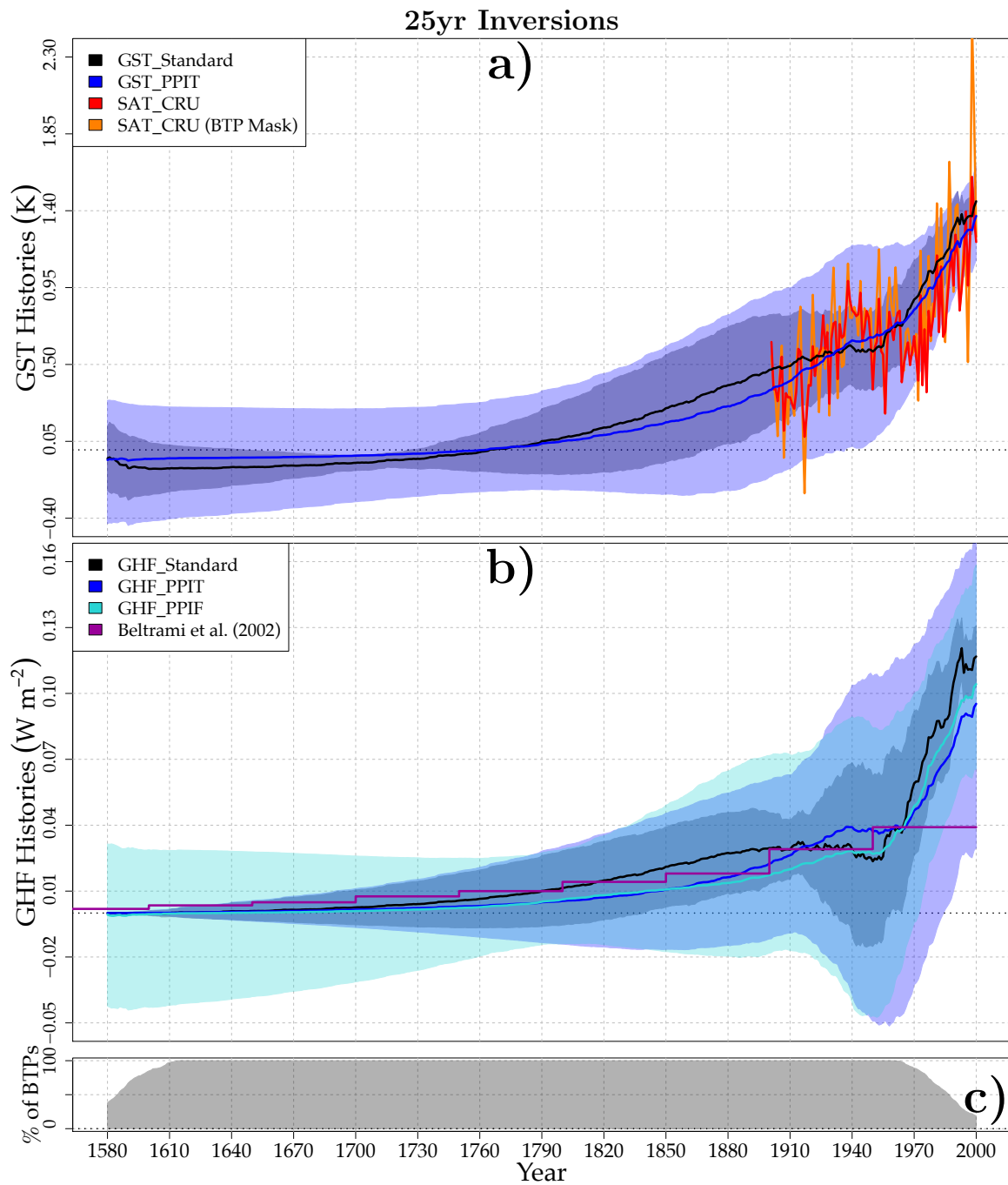


Figure 3. Global ground surface temperature histories (a) and global ground heat flux histories at the surface (b) from borehole temperature profiles using the Standard approach (black), and the new PPI approach applied to temperature profiles (PPIT, blue) and the [..⁹⁸] corresponding heat flux profiles (PPIF, light blue). All inversions were performed using a 25 yr [..⁹⁹] step change model. (c) Percentage of total borehole inversions with time. Surface air temperature anomalies relative to 1961-1990 CE from CRU data (SAT_CRU) are also displayed, including results from the entire database (red) and results from locations and dates containing borehole inversions (orange). The CRU series have been adjusted to have the same mean than the results [..¹⁰⁰] of the GST_Standard [..¹⁰¹] ensemble for the period 1950-1970 CE.

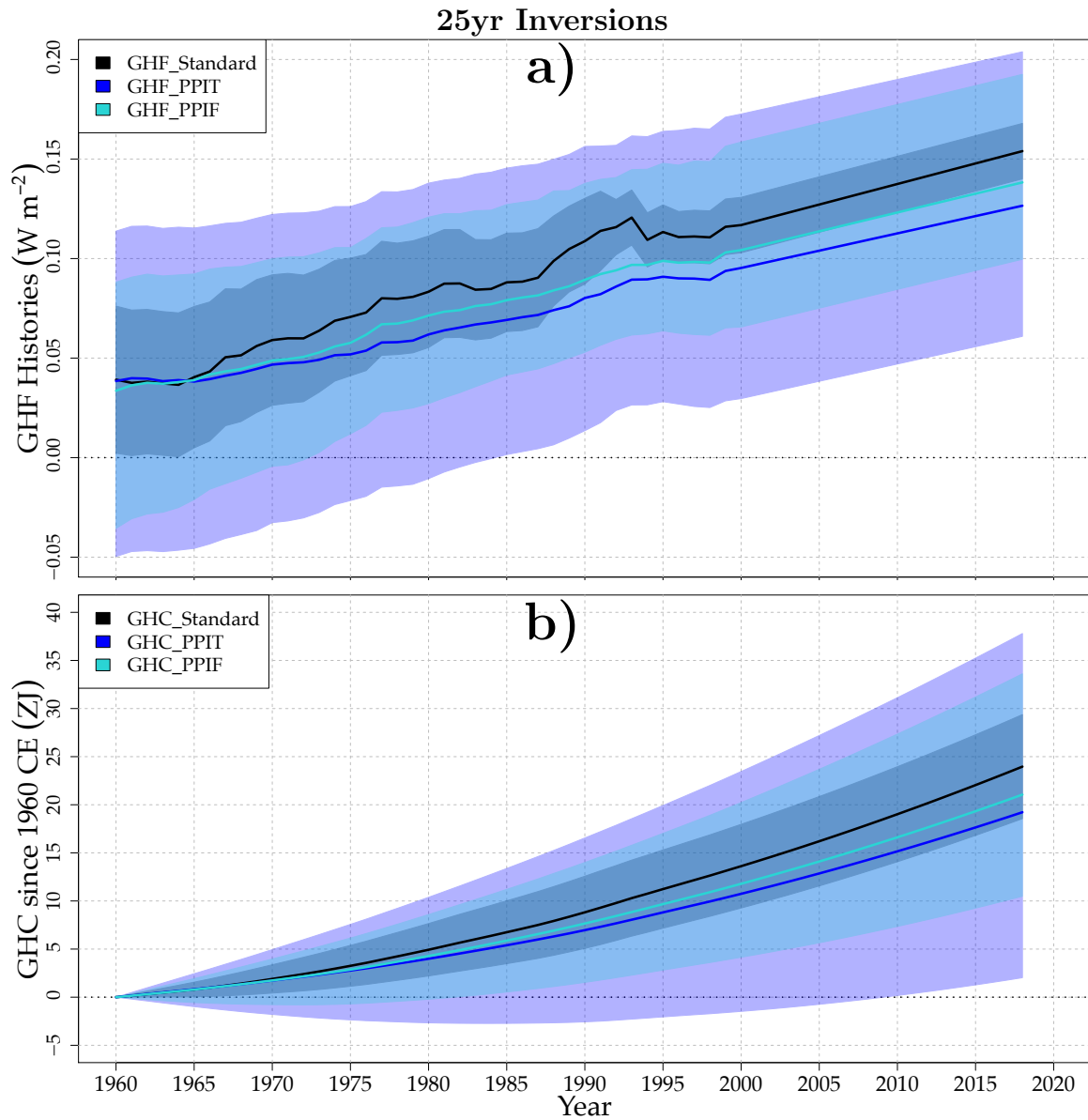


Figure 4. Global ground heat flux histories (a) and ground heat content accumulated since 1960 CE (b) from borehole temperature profiles using the Standard approach (black), and the new PPI approach applied to temperature profiles (PPIT, blue) and [¹⁰²] the corresponding heat flux profiles (PPIF, light blue). All inversions were performed using a 25 yr inversion model. Data since 2001 CE to 2018 CE are extrapolated using the trend for the period 1971-2000 CE.